Computing distances and means between manifold-valued curves

in the SRV framework

Alice Le Brigant
Marc Arnaudon
Frédéric Barbaresco

21 July 2016

Table of contents

Table of contents

Some motivations for studying curves in a manifold

- Statistical analysis of trajectories $\to$ plane curves or S^2-valued curves

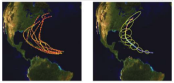

(a) Hurricane tracks[1]

(b) Car trajectories at a crossroads[1]

- Image analysis and computer vision $\to$ curves in the space of SPDMs

(c) Hand-gesture classification[2]

(d) Visual-speed recognition[2]

- Signal processing $\to$ curves in the space of Toeplitz HPDMs, representation in $\mathbb{H}$

(e) Non stationarity in radar applications

1. Images from [Su, Kurtek, Klassen, Srivastava 2014], 2. Images from [Zhang, Su, Klassen, Le, Srivastava 2015]

Information Geometry

- Geometric approach : see probability distributions as points in a manifold

  Family of probability densities $\{f(\cdot,\theta), \theta \in \Theta\}$
  Each $f(\cdot,\theta)$ is represented by parameter θ in manifold Θ

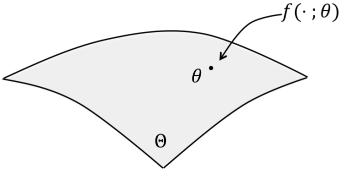

- Riemannian structure : Fisher Information metric

  It is given by the Fisher Information matrix $I(\theta)$

$$g_{ij}(\theta) = I(\theta)_{ij} = \mathbb{E}_\theta\left[\left(\frac{\partial}{\partial\theta_i}\ln f(X;\theta)\right)\left(\frac{\partial}{\partial\theta_j}\ln f(X;\theta)\right)\right] \qquad \theta = (\theta_1,\ldots,\theta_p)$$

Fisher Information

In parameter estimation,

- measures the "amount of information" contained in the data

  goal : estimate θ using i.i.d. samples $X_1, \dots, X_n \sim f(\cdot, \theta)$.
  "$I(\theta)$ = amount of information contained in samples $X_1, \dots, X_n$"

  e.g. $f(\cdot, \theta) = \mathcal{N}(\theta, \sigma^2)$ with σ^2 known $\Longrightarrow$ $I(\theta) = \frac{n}{\sigma^2}$

- gives a limit to the precision at which we can estimate θ

  Thm (Cramer-Rao bound) : For any unbiased estimator T of parameter θ,

$$\mathrm{Var}\, T = \mathbb{E}_\theta[(T(X) - \theta)^2] \geq I(\theta)^{-1}.$$

  e.g. $X_1, \dots, X_n \sim \mathcal{N}(\theta, \sigma^2)$, σ^2 known, $T(X_1, \dots, X_n) = \bar{X}_n = \frac{1}{n}\sum X_i$.
  $\mathbb{E}_\theta\left[(\bar{X}_n - \theta)^2\right] = \frac{\sigma^2}{n} = \frac{1}{I(\theta)} \Longrightarrow \bar{X}_n$ minimum variance unbiased estimator.

Statistical manifold

Space of parameters Θ + Fisher Information metric = Statistical manifold

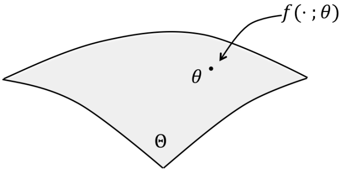

Ex : For univariate Gaussian distributions $\mathcal{N}(\mu,\sigma^2)$,

Fisher geometry amounts to hyperbolic geometry.

The space of parameters (μ,σ) equipped with the Fisher Information metric is in bijection with the hyperbolic upper-half plane via the change of variables $(\mu,\sigma) \mapsto (\frac{\mu}{\sqrt{2}},\sigma)$.

Hyperbolic Fisher geometry of Gaussians

- Hyperbolic upper-half plane $\mathbb{H}$

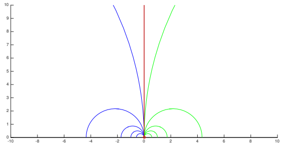

$\mathbb{H}$ is one of the representations of 2-dim. hyperbolic geometry

$$ds^2 = \frac{dx^2 + dy^2}{y^2}$$

- Euclidean distance is unsuitable to compare univariate Gaussian distributions in the upper half-plane

[Costa, Santos, Strapasson, 2014]

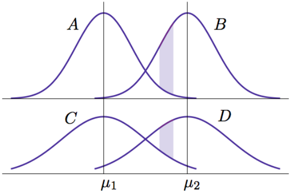

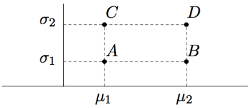

Our setting : spectral estimation in signal processing

- Given : vector $(X_1, \ldots, X_N) \in \mathbb{C}^N$ of radar data

- Aim : study temporal modulations of underlying signal

  – Assume : underlying process is locally stationary & Gaussian

  – For each stationary portion, estimate maximum entropy spectrum = AR spectrum [Burg'75]

  – 2^{nd}-order statistics of each spectrum can be equivalently represented by covariance matrix Σ or the *reflection coefficients* of the AR model

$$\mathcal{T}_n \ni \ \Sigma \xleftrightarrow{\text{bij.}} (P, \mu_1, \ldots, \mu_{n-1}) \ \in \mathbb{R}_+^* \times D^{n-1}$$

  $\mathcal{T}_n$ = space of Toeplitz HPDM, D = complex disk.

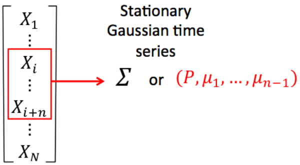

  – When induced with the dual of the Fisher Information metric, the space of reflection coeff. $\mathbb{R}_+^* \times D^{n-1}$ becomes the product manifold $\mathbb{R}_+^* \times \mathbb{D}^{n-1}$, where $\mathbb{D}$ = Poincaré disk. [Barbaresco'09]

- We obtain curves in the Poincaré disk

Table of contents

The Riemannian setting

- Riemannian manifold $(M, \langle\cdot,\cdot\rangle)$ (e.g. hyperbolic upper half plane $\mathbb{H}$)
- Space of open curves (immersions) in M
$$\mathcal{C} = \mathrm{Imm}([0,1], M) = \left\{c \in C^\infty([0,1], M),\, c'(t) \neq 0 \forall t \in [0,1]\right\}$$
which we equip with a Riemannian metric G
- We can compare two curves using the geodesic distance
$$\mathrm{dist}_G(c_0, c_1) = \inf_{c(0,\cdot)=c_0, c(1,\cdot)=c_1} \int_0^1 G\left(\frac{\partial c}{\partial s}, \frac{\partial c}{\partial s}\right) \mathrm{d}s$$
and average several curves using the Fréchet mean or median
$$c_m = \underset{c}{\mathrm{argmin}} \sum_{i=1}^n \mathrm{dist}_G^k(c_i, c) \qquad \begin{array}{l} k = 1 : \text{median} \\ k = 2 : \text{mean} \end{array}$$

Notations

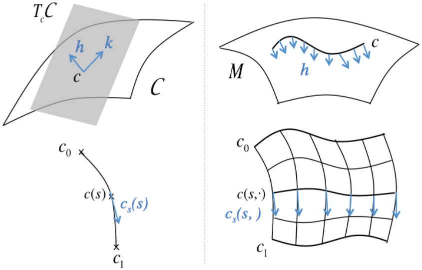

- A tangent vector $h \in T_c\mathcal{C}$ is a vector field along the curve c in M.
- A path $s \mapsto c(s)$ in $\mathcal{C}$ is a "deformation surface" $(s,t) \mapsto c(s,t)$ in M.
  - s : time parameter of a path in $\mathcal{C}$
  - t : time parameter of a curve in M
- A diffeomorphism $\phi \in$ Diff([0,1] is a reparametrization of c

Reparameterization invariance

We want a metric that verifies the equivariance property

$$G_{c\circ\phi}(h\circ\phi, k\circ\phi) = G_c(h,k) \qquad \forall\phi\in \mathrm{Diff}^+([0,1])$$

Reparameterization invariance

We want a metric that verifies the equivariance property

$$G_{c\circ\phi}(h\circ\phi, k\circ\phi) = G_c(h,k) \qquad \forall\phi \in \mathrm{Diff}^+([0,1])$$

- The distance between two curves is the same if we reparameterize them the same way

$$\mathrm{dist}(c_0\circ\phi, c_1\circ\phi) = \mathrm{dist}(c_0, c_1) \quad \forall\phi$$

Reparameterization invariance

We want a metric that verifies the equivariance property

$$G_{c\circ\phi}(h\circ\phi, k\circ\phi) = G_c(h,k) \qquad \forall\phi \in \mathrm{Diff}^+([0,1])$$

- The distance between two curves is the same if we reparameterize them the same way

$$\mathrm{dist}(c_0\circ\phi, c_1\circ\phi) = \mathrm{dist}(c_0, c_1) \quad \forall\phi$$

- We induce a Riemannian metric on the shape space $\mathcal{S} = \mathcal{C}/\mathrm{Diff}^+([0,1])$

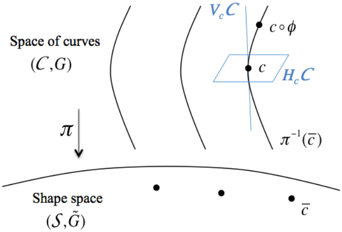

"Formal" principle bundle structure $\pi : \mathcal{C} \to \mathcal{S}$

$$V\mathcal{C} = \ker(T\pi),\ H\mathcal{C} = (V\mathcal{C})^{\perp_G}$$

The geodesics of $\mathcal{S}$ are the horizontal geodesics of $\mathcal{C}$

The induced distance on $\mathcal{S}$ is

$$\mathrm{dist}_{\mathcal{S}}(\bar{c}_0, \bar{c}_1) = \inf\left\{\mathrm{dist}(c_0, c_1\circ\phi) \,|\, \phi \in \mathrm{Diff}^+([0,1])\right\}$$

The problem with the L^2 metric

The most natural choice : L^2-metric

$$G_c(h,k) = \int_0^1 \langle h(t), k(t) \rangle \, \|c'(t)\| \mathrm{d}t.$$

Problem : induces a vanishing distance on the shape space [Michor, Mumford, 2006]

1. $\mathrm{dist}(\bar{c}_0, \bar{c}_1) = L^{hor}(c)$ where $c =$ geodesic between c_0 and c_1
2. for the L^2 metric, $h^{hor} = h^{\perp} := \langle h, n \rangle n$ where $n =$ unit orthogonal vector to speed c'

$\rightarrow \mathrm{dist}(\bar{c}_0, \bar{c}_1)$ depends on the square of the normal component $c_s^{\perp}$ of the deformation speed.

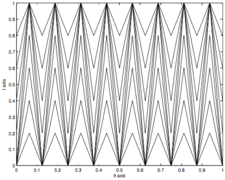

Figure: Illustration from [Michor, Mumford, 2006]

In this example, $c_s(s,\cdot)^{\perp}$ is inversely proportional to the length of $c(s,\cdot)$, which grows with the number of "teeth".

$\rightarrow \mathrm{dist}(\bar{c}_0, \bar{c}_1)$ can be as small as we want.

The SRV framework

$M = \mathbb{R}^d$

- We add terms that involve higher order derivatives : Sobolev metrics.

$$\text{e.g.} \qquad G_c(h,k) = \int \langle h,k\rangle + \langle D_\ell h, D_\ell k\rangle \, \mathrm{d}\ell$$

with $D_\ell h := h'/\|c'\|$ and $d\ell = \|c'(t)\|\mathrm{d}t$.

- If you put different weights on the normal and tangential parts : "elastic metrics"

$$G_c^{a,b}(h,k) = \int a^2 \langle D_\ell h^N, D_\ell k^N \rangle + b^2 \langle D_\ell h^T, D_\ell k^T \rangle \, \mathrm{d}\ell,$$

$D_\ell h^T := \langle D_\ell h, v\rangle v$ with $v = c'/\|c'\|$
$D_\ell h^N := D\ell h - D_\ell h^T$

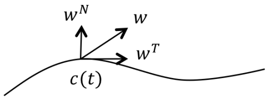

a : degree of bending of the curve
b : degree of stretching

[Mio, Srivastava, Joshi 2006]

The SRV framework

$M = \mathbb{R}^d$

- Particularly interesting for $a = 1$, $b = 1/2$

$$G_c(h,k) = \int \langle D_\ell h^N, D_\ell k^N \rangle + \frac{1}{4} \langle D_\ell h^T, D_\ell k^T \rangle \, \mathrm{d}\ell$$

pullback of the L^2-metric via the "Square Root Velocity Function" (SRVF) $R : c \mapsto c' / \sqrt{\|c'\|}$

$$G_c(h,k) = \int \langle T_c R(h), T_c R(k) \rangle \, \mathrm{d}t$$

R verifies $T_{c\circ\phi} R(h \circ \phi) = \|\phi'\|^{1/2} T_c R(h) \circ \phi$, which guaranties the equivariance property.

[Srivastava, Klassen, Joshi, Jermyn 2011], [Younes 1998].

- The SRV framework can be extended to any $a, b \in \mathbb{R}_+$ satisfying $4b^2 \geq a^2$, however the formulas get rather involved.

[Bauer, Bruveris, Marsland, Michor 2012]

Our generalization to curves in any manifold M

M manifold

- We consider the Riemannian metric

$$G_c(h,k) = \langle h(0), k(0)\rangle + \int_0^1 \langle \nabla_\ell h^N, \nabla_\ell k^N \rangle + \frac{1}{4}\langle \nabla_\ell h^T, \nabla_\ell k^T \rangle \mathrm{d}\ell$$

$\nabla_\ell h := \nabla_{c'} h / \|c'\|$, $d\ell = \|c'(t)\|\mathrm{d}t$,

$\nabla_\ell h^T := \langle \nabla_\ell h, v\rangle v$ with $v = c'/\|c'\|$ and $\nabla_\ell h^N := \nabla_\ell h - D_\ell h^T$.

- It can be obtained as the pullback of the metric on $T\mathcal{C}$

$$\tilde{G}(\eta_s(s), \eta_s(s)) = \|c_s(s,0)\|^2 + \int_0^1 \|\nabla_s v(s,t)\|^2 \mathrm{d}t$$

where $s \mapsto \eta(s,\cdot) = (c(s,\cdot), v(s,\cdot))$ is a path in $T\mathcal{C}$.

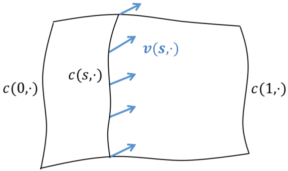

Our generalization to curves in any manifold M

M manifold

- Induced distance

$$\operatorname{dist}(c_0, c_1) = \inf_c \int_0^1 \sqrt{\|c_s(s,0)\|^2 + \int_0^1 \|\nabla_s q(s,t)\|^2 \,\mathrm{d}t} \,\mathrm{d}s,$$

where $q = c_t / \sqrt{\|c_t\|}$ is the the SRV representation of c.

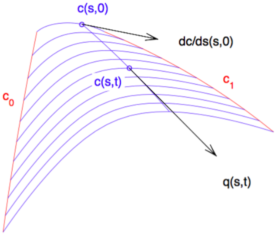

- Differs from the generalization of Zhang et. al. with the TSRVF
  - The information of each curve is not concentrated in a single point (e.g. its origin)
  - The energy of the deformation between two curves takes into account the curvature of the manifold along the entire "deformation surface"
  - This distance relates to a Sobolev metric

  They coincide when M is flat.

  [Zhang, Su, Klassen, Le, Srivastava 2015]

The geodesic equations

- The geodesics are the paths that minimize the energy

$$E(c) := \frac{1}{2}\int G_{c(s)}\left(c_s(s), c_s(s)\right) \mathrm{d}s.$$

The geodesic equations

- The geodesics are the paths that minimize the energy

$$E(c) := \frac{1}{2} \int G_{c(s)}\left(c_s(s), c_s(s)\right) \mathrm{d}s.$$

- To find the geodesic between c_0 and c_1, consider a path of curves c

$$s \mapsto c(s,\cdot) : c(0,\cdot) = c_0, c(1,\cdot) = c_1$$

and a variation of c preserving the end points

$$\hat{c} : \begin{cases} (-\varepsilon,\varepsilon) \to \mathcal{C} \\ a \mapsto \hat{c}(a,\cdot,\cdot) \end{cases}$$

s.t. $\hat{c}(0,s,t) = c(s,t)$, $\hat{c}(a,0,t) = c_0(t)$ and $\hat{c}(a,1,t) = c_1(t)$

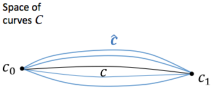

The geodesic equations

- The geodesics are the paths that minimize the energy

$$E(c) := \frac{1}{2}\int G_{c(s)}\left(c_s(s), c_s(s)\right) \mathrm{d}s.$$

- To find the geodesic between c_0 and c_1, consider a path of curves c

  $s \mapsto c(s,\cdot) : c(0,\cdot) = c_0, c(1,\cdot) = c_1$

  and a variation of c preserving the end points

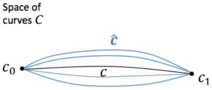

$$\hat{c} : \begin{cases} (-\varepsilon,\varepsilon) \to \mathcal{C} \\ a \mapsto \hat{c}(a,\cdot,\cdot) \end{cases}$$

s.t. $\hat{c}(0,s,t) = c(s,t)$, $\hat{c}(a,0,t) = c_0(t)$ and $\hat{c}(a,1,t) = c_1(t)$

The energy of this variation is $\hat{E} : (-\varepsilon,\varepsilon) \to \mathbb{R}_+$

$$\hat{E}(a) := E\left(\hat{c}(a,\cdot,\cdot)\right) = \frac{1}{2}\int G\left(\hat{c}_s(a,s,\cdot), \hat{c}_s(a,s,\cdot)\right) \mathrm{d}s$$

and we want $s \mapsto c(s,\cdot)$ s.t. $\left.\frac{d}{da}\right|_{a=0} \hat{E}(a) = 0$ for any variation $\hat{c}$.

The geodesic equations

- In our case, we have

$$\hat{E}(a) = \frac{1}{2}\int \langle \hat{c}_s(a,s,0), \hat{c}_s(a,s,0) \rangle \mathrm{d}s + \int\int \langle \nabla_s \hat{q}(s,t), \nabla_s \hat{q}(s,t) \rangle \mathrm{d}t\,\mathrm{d}s,$$

$$\hat{E}'(a) = \int \langle \nabla_a \hat{c}_s(a,s,0), \hat{c}_s(a,s,0) \rangle \,\mathrm{d}s + \int\int \langle \nabla_a \nabla_s \hat{q}(a,s,t), \nabla_s \hat{q}(a,s,t) \rangle \,\mathrm{d}t\,\mathrm{d}s,$$

which can be written for $a = 0$

$$\int_0^1 \langle\, \nabla_s c_s(s,0) + r(s,0)\,,\, \hat{c}_a(0,s,0)\,\rangle \mathrm{d}s + \int_0^1 \int_0^1 \langle\, \nabla_s \nabla_s q(s,t) + \|q\|\,(r + r^T)\,(s,t)\,,\, \nabla_a \hat{q}(0,s,t)\,\rangle \,\mathrm{d}t\,\mathrm{d}s = 0,$$

with $r(s,t) = \int_t^1 \mathcal{R}(q, \nabla_s q) c_s(s,\tau)^{\tau,t} \mathrm{d}\tau.$

The geodesic equations

- In our case, we have

$$\begin{aligned}\hat{E}(a) &= \frac{1}{2}\int \langle \hat{c}_s(a,s,0), \hat{c}_s(a,s,0)\rangle \mathrm{d}s + \int\int \langle \nabla_s \hat{q}(s,t), \nabla_s \hat{q}(s,t)\rangle \mathrm{d}t\,\mathrm{d}s,\\ \hat{E}'(a) &= \int \langle \nabla_a \hat{c}_s(a,s,0), \hat{c}_s(a,s,0)\rangle \mathrm{d}s + \int\int \langle \nabla_a \nabla_s \hat{q}(a,s,t), \nabla_s \hat{q}(a,s,t)\rangle \mathrm{d}t\,\mathrm{d}s,\end{aligned}$$

which can be written for $a = 0$

$$\int_0^1 \langle\, \nabla_s c_s(s,0) + r(s,0)\,,\, \hat{c}_a(0,s,0)\,\rangle \mathrm{d}s + \int_0^1 \int_0^1 \langle\, \nabla_s \nabla_s q(s,t) + \|q\|\left(r + r^T\right)(s,t)\,,\, \nabla_a \hat{q}(0,s,t)\,\rangle \mathrm{d}t\,\mathrm{d}s = 0,$$

with $r(s,t) = \int_t^1 \mathcal{R}(q, \nabla_s q) c_s(s,\tau)^{\tau,t} \mathrm{d}\tau.$

The geodesic equations

- In our case, we have

$$\hat{E}(a) = \frac{1}{2}\int \langle \hat{c}_s(a,s,0), \hat{c}_s(a,s,0) \rangle \mathrm{d}s + \int\int \langle \nabla_s \hat{q}(s,t), \nabla_s \hat{q}(s,t) \rangle \mathrm{d}t\,\mathrm{d}s,$$

$$\hat{E}'(a) = \int \langle \nabla_a \hat{c}_s(a,s,0), \hat{c}_s(a,s,0) \rangle \,\mathrm{d}s + \int\int \langle \nabla_a \nabla_s \hat{q}(a,s,t), \nabla_s \hat{q}(a,s,t) \rangle \,\mathrm{d}t\,\mathrm{d}s,$$

which can be written for $a = 0$

$$\int_0^1 \langle\, \nabla_s c_s(s,0) + r(s,0)\,,\, \hat{c}_a(0,s,0)\, \rangle \mathrm{d}s + \int_0^1 \int_0^1 \langle\, \nabla_s \nabla_s q(s,t) + \|q\| \left(r + r^T\right)(s,t)\,,\, \nabla_a \hat{q}(0,s,t)\, \rangle \,\mathrm{d}t\,\mathrm{d}s = 0,$$

with $r(s,t) = \int_t^1 \mathcal{R}(q, \nabla_s q) c_s(s,\tau)^{\tau,t} \mathrm{d}\tau.$

The geodesic equations

- In our case, we have

$$\hat{E}(a) = \frac{1}{2}\int \langle \hat{c}_s(a,s,0), \hat{c}_s(a,s,0)\rangle \mathrm{d}s + \int\int \langle \nabla_s \hat{q}(s,t), \nabla_s \hat{q}(s,t)\rangle \mathrm{d}t\,\mathrm{d}s,$$

$$\hat{E}'(a) = \int \langle \nabla_a \hat{c}_s(a,s,0), \hat{c}_s(a,s,0)\rangle \,\mathrm{d}s + \int\int \langle \nabla_a \nabla_s \hat{q}(a,s,t), \nabla_s \hat{q}(a,s,t)\rangle \,\mathrm{d}t\,\mathrm{d}s,$$

which can be written for $a=0$

$$\int_0^1 \langle\, \nabla_s c_s(s,0) + r(s,0)\,,\, \hat{c}_a(0,s,0)\,\rangle \mathrm{d}s + \int_0^1\int_0^1 \langle\, \nabla_s\nabla_s q(s,t) + \|q\|\,(r + r^T)\,(s,t)\,,\, \nabla_a \hat{q}(0,s,t)\,\rangle\,\mathrm{d}t\,\mathrm{d}s = 0,$$

with $r(s,t) = \int_t^1 \mathcal{R}(q, \nabla_s q) c_s(s,\tau)^{\tau,t} \mathrm{d}\tau.$

- We obtain the equations describing the shortest deformation of one curve into another

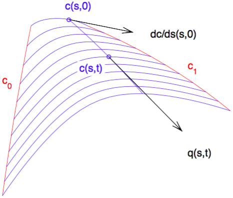

$$(*) \quad \begin{cases} \nabla_s c_s(s,0) + r(s,0) = 0 \quad \forall s \\ \nabla_s \nabla_s q(s,t) + \|q(s,t)\|\,\left(r(s,t) + r(s,t)^T\right) = 0 \quad \forall t,s \end{cases}$$

avec $r(s,t) = \int_t^1 \mathcal{R}(q, \nabla_s q) c_s(s,\tau)^{\tau,t} \mathrm{d}\tau.$

Table of contents

Discretization of our model

Continuous model	Discrete model

Continuous model

Space of curves $\mathcal{C}$

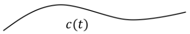

Path in $\mathcal{C}$: $\quad s \mapsto c(s,\cdot)$

Riemannian metric

$$G_c(c_s(s), c_s(s)) = \|c_s(s,0)\|^2 + \int_0^1 \|\nabla_s q(s,t)\|^2 \mathrm{d}t$$

Geodesic equations

$$\nabla_s c_s(s,0) + r(s,0) = 0$$
$$\nabla_s \nabla_s q(s,t) + \|q(s,t)\| \left(r(s,t) + r(s,t)^T \right) = 0$$

with $\; r(s,t) = \int_t^1 \mathcal{R}(q, \nabla_s q) c_s(s,\tau)^{\tau,t} \mathrm{d}\tau.$

Discrete model

Space of discretized curves M^{n+1}

Path in M^{n+1} : $\quad s \mapsto \alpha(s) = (p_0(s), \dots, p_n(s))$

Riemannian metric

$$G_c(\alpha'(s), \alpha'(s)) = \|p_0'(s)\|^2 + \frac{1}{n} \sum_{k=0}^{n-1} \|\nabla_s q_k(s,t)\|^2$$

Geodesic equations

$$\nabla_s {p_0}' + \frac{1}{n} \sum_{k=0}^{n-1} f_0 \circ \cdots \circ f_{k-1} \left(\mathcal{R}(q_k, \nabla_s q_k) {p_k}' \right) = 0,$$
$$\nabla_s \nabla_s q_k + \frac{1}{n} \sum g_k \circ f_{k+1} \circ \cdots \circ f_{\ell-1} \left(\mathcal{R}(q_\ell, \nabla_s q_\ell) {p_\ell}' \right) = 0.$$

with $f_0 \circ \cdots \circ f_{k-1}(w_k) \to w_k^{p_k, p_0}$

$g_k \circ f_{k+1} \circ \cdots \circ f_{\ell-1}(w_\ell) \to \|q_k\| (w_\ell^{p_\ell, p_k} + (w_\ell^{p_\ell, p_k})^T).$

Exponential map

Gives an approximation of the geodesic starting from c_0 at speed u_0

We solve the system $(*)$:

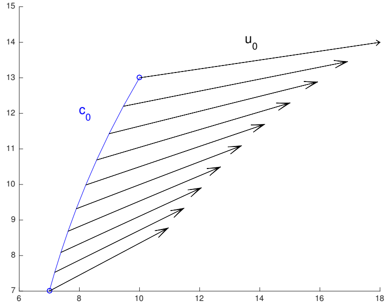

Simulation in the hyperbolic half-plane

at time s, if $c(s,\cdot)$ and $c_s(s,\cdot)$ are known, we propagate to time $s+\varepsilon$ using

$$\begin{aligned} c(s+\varepsilon,t) &= \exp^M_{c(s,t)}(\varepsilon c_s(s,\varepsilon)) \quad \forall t \\ c_s(s+\varepsilon,t) &= c_s(s,t)+\varepsilon\nabla_s c_s(s,t) \quad \forall t, \end{aligned}$$

$\exp_{c(s,t)}(\varepsilon c_s(s,\varepsilon))$: point obtained by following the geodesic of M starting from $c(s,t)$ at speed $\varepsilon c_s(s,\varepsilon)$,

$\nabla_s c_s$ can be deduced from $(*)$.

Exponential map

Gives an approximation of the geodesic starting from c_0 at speed u_0

We solve the system $(*)$:

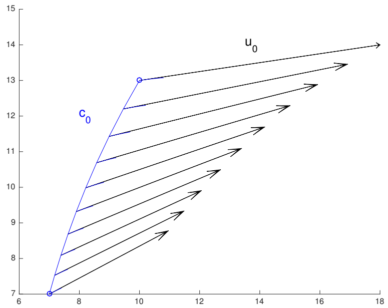

Simulation in the hyperbolic half-plane

at time s, if $c(s,\cdot)$ and $c_s(s,\cdot)$ are known, we propagate to time $s+\varepsilon$ using

$$\begin{aligned} c(s+\varepsilon,t) &= \exp^M_{c(s,t)}(\varepsilon c_s(s,\varepsilon)) \quad \forall t \\ c_s(s+\varepsilon,t) &= c_s(s,t)+\varepsilon\nabla_s c_s(s,t) \quad \forall t, \end{aligned}$$

$\exp_{c(s,t)}(\varepsilon c_s(s,\varepsilon))$: point obtained by following the geodesic of M starting from $c(s,t)$ at speed $\varepsilon c_s(s,\varepsilon)$,

$\nabla_s c_s$ can be deduced from $(*)$.

Exponential map

Gives an approximation of the geodesic starting from c_0 at speed u_0

We solve the system $(*)$:

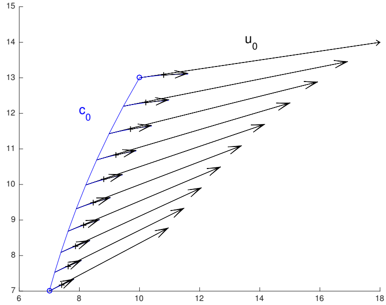

Simulation in the hyperbolic half-plane

at time s, if $c(s,\cdot)$ and $c_s(s,\cdot)$ are known, we propagate to time $s+\varepsilon$ using

$$\begin{aligned} c(s+\varepsilon,t) &= \exp^M_{c(s,t)}(\varepsilon c_s(s,\varepsilon)) \quad \forall t \\ c_s(s+\varepsilon,t) &= c_s(s,t)+\varepsilon\nabla_s c_s(s,t) \quad \forall t, \end{aligned}$$

$\exp_{c(s,t)}(\varepsilon c_s(s,\varepsilon))$: point obtained by following the geodesic of M starting from $c(s,t)$ at speed $\varepsilon c_s(s,\varepsilon)$,

$\nabla_s c_s$ can be deduced from $(*)$.

Exponential map

Gives an approximation of the geodesic starting from c_0 at speed u_0

We solve the system $(*)$:

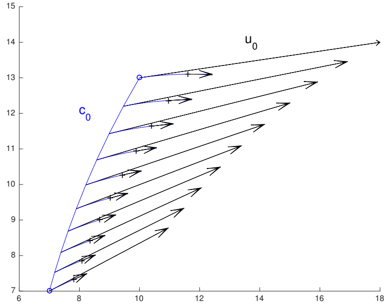

Simulation in the hyperbolic half-plane

at time s, if $c(s,\cdot)$ and $c_s(s,\cdot)$ are known, we propagate to time $s+\varepsilon$ using

$$\begin{aligned} c(s+\varepsilon,t) &= \exp^M_{c(s,t)}(\varepsilon c_s(s,\varepsilon)) \quad \forall t \\ c_s(s+\varepsilon,t) &= c_s(s,t)+\varepsilon\nabla_s c_s(s,t) \quad \forall t, \end{aligned}$$

$\exp_{c(s,t)}(\varepsilon c_s(s,\varepsilon))$: point obtained by following the geodesic of M starting from $c(s,t)$ at speed $\varepsilon c_s(s,\varepsilon)$,

$\nabla_s c_s$ can be deduced from $(*)$.

Exponential map

Gives an approximation of the geodesic starting from c_0 at speed u_0

We solve the system $(*)$:

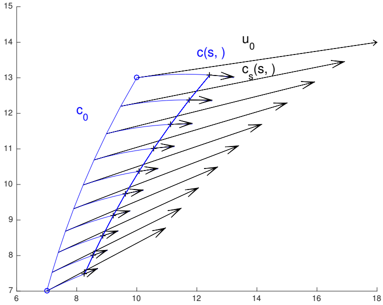

Simulation in the hyperbolic half-plane

at time s, if $c(s,\cdot)$ and $c_s(s,\cdot)$ are known, we propagate to time $s+\varepsilon$ using

$$\begin{aligned} c(s+\varepsilon,t) &= \exp^M_{c(s,t)}(\varepsilon c_s(s,\varepsilon)) \quad \forall t \\ c_s(s+\varepsilon,t) &= c_s(s,t)+\varepsilon\nabla_s c_s(s,t) \quad \forall t, \end{aligned}$$

$\exp_{c(s,t)}(\varepsilon c_s(s,\varepsilon))$: point obtained by following the geodesic of M starting from $c(s,t)$ at speed $\varepsilon c_s(s,\varepsilon)$,

$\nabla_s c_s$ can be deduced from $(*)$.

Exponential map

Gives an approximation of the geodesic starting from c_0 at speed u_0

We solve the system $(*)$:

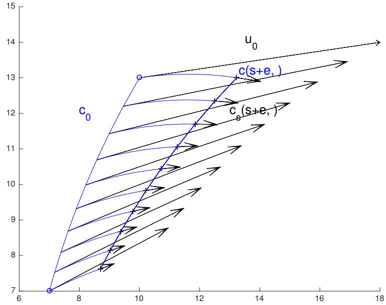

Simulation in the hyperbolic half-plane

at time s, if $c(s,\cdot)$ and $c_s(s,\cdot)$ are known, we propagate to time $s+\varepsilon$ using

$$
\begin{aligned}
c(s+\varepsilon,t) &= \exp^M_{c(s,t)}(\varepsilon c_s(s,\varepsilon)) \quad \forall t \\
c_s(s+\varepsilon,t) &= c_s(s,t)+\varepsilon\nabla_s c_s(s,t) \quad \forall t,
\end{aligned}
$$

$\exp_{c(s,t)}(\varepsilon c_s(s,\varepsilon))$: point obtained by following the geodesic of M starting from $c(s,t)$ at speed $\varepsilon c_s(s,\varepsilon)$,

$\nabla_s c_s$ can be deduced from $(*)$.

Exponential map

Gives an approximation of the geodesic starting from c_0 at speed u_0

We solve the system $(*)$:

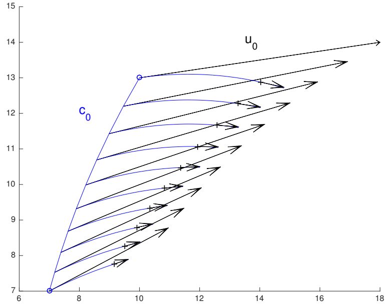

Simulation in the hyperbolic half-plane

at time s, if $c(s,\cdot)$ and $c_s(s,\cdot)$ are known, we propagate to time $s+\varepsilon$ using

$$\begin{aligned} c(s+\varepsilon,t) &= \exp^M_{c(s,t)}(\varepsilon c_s(s,\varepsilon)) \quad \forall t \\ c_s(s+\varepsilon,t) &= c_s(s,t)+\varepsilon\nabla_s c_s(s,t) \quad \forall t, \end{aligned}$$

$\exp_{c(s,t)}(\varepsilon c_s(s,\varepsilon))$: point obtained by following the geodesic of M starting from $c(s,t)$ at speed $\varepsilon c_s(s,\varepsilon)$,

$\nabla_s c_s$ can be deduced from $(*)$.

Exponential map

Gives an approximation of the geodesic starting from c_0 at speed u_0

We solve the system $(*)$:

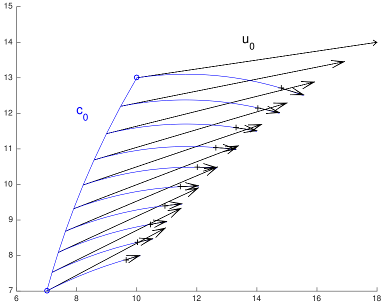

Simulation in the hyperbolic half-plane

at time s, if $c(s,\cdot)$ and $c_s(s,\cdot)$ are known, we propagate to time $s+\varepsilon$ using

$$\begin{aligned} c(s+\varepsilon,t) &= \exp^M_{c(s,t)}(\varepsilon c_s(s,\varepsilon)) \quad \forall t \\ c_s(s+\varepsilon,t) &= c_s(s,t)+\varepsilon\nabla_s c_s(s,t) \quad \forall t, \end{aligned}$$

$\exp_{c(s,t)}(\varepsilon c_s(s,\varepsilon))$: point obtained by following the geodesic of M starting from $c(s,t)$ at speed $\varepsilon c_s(s,\varepsilon)$,

$\nabla_s c_s$ can be deduced from $(*)$.

Exponential map

Gives an approximation of the geodesic starting from c_0 at speed u_0

We solve the system $(*)$:

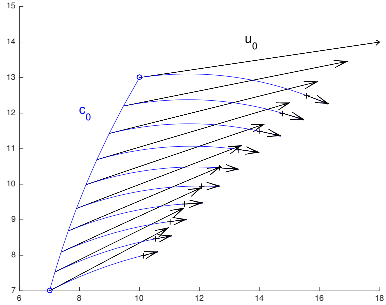

Simulation in the hyperbolic half-plane

at time s, if $c(s,\cdot)$ and $c_s(s,\cdot)$ are known, we propagate to time $s+\varepsilon$ using

$$\begin{aligned} c(s+\varepsilon,t) &= \exp^M_{c(s,t)}(\varepsilon c_s(s,\varepsilon)) \quad \forall t \\ c_s(s+\varepsilon,t) &= c_s(s,t)+\varepsilon\nabla_s c_s(s,t) \quad \forall t, \end{aligned}$$

$\exp_{c(s,t)}(\varepsilon c_s(s,\varepsilon))$: point obtained by following the geodesic of M starting from $c(s,t)$ at speed $\varepsilon c_s(s,\varepsilon)$,

$\nabla_s c_s$ can be deduced from $(*)$.

Exponential map

Gives an approximation of the geodesic starting from c_0 at speed u_0

We solve the system $(*)$:

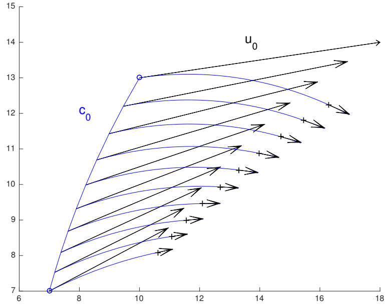

Simulation in the hyperbolic half-plane

at time s, if $c(s,\cdot)$ and $c_s(s,\cdot)$ are known, we propagate to time $s+\varepsilon$ using

$$\begin{aligned} c(s+\varepsilon,t) &= \exp^M_{c(s,t)}(\varepsilon c_s(s,\varepsilon)) \quad \forall t \\ c_s(s+\varepsilon,t) &= c_s(s,t)+\varepsilon\nabla_s c_s(s,t) \quad \forall t, \end{aligned}$$

$\exp_{c(s,t)}(\varepsilon c_s(s,\varepsilon))$: point obtained by following the geodesic of M starting from $c(s,t)$ at speed $\varepsilon c_s(s,\varepsilon)$,

$\nabla_s c_s$ can be deduced from $(*)$.

Exponential map

Gives an approximation of the geodesic starting from c_0 at speed u_0

We solve the system $(*)$:

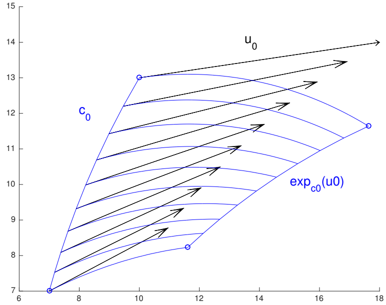

Simulation in the hyperbolic half-plane

at time s, if $c(s,\cdot)$ and $c_s(s,\cdot)$ are known, we propagate to time $s+\varepsilon$ using

$$\begin{aligned} c(s+\varepsilon,t) &= \exp^M_{c(s,t)}(\varepsilon c_s(s,\varepsilon)) \quad \forall t \\ c_s(s+\varepsilon,t) &= c_s(s,t)+\varepsilon\nabla_s c_s(s,t) \quad \forall t, \end{aligned}$$

$\exp_{c(s,t)}(\varepsilon c_s(s,\varepsilon))$: point obtained by following the geodesic of M starting from $c(s,t)$ at speed $\varepsilon c_s(s,\varepsilon)$,

$\nabla_s c_s$ can be deduced from $(*)$.

Geodesic shooting

Gives an approximation of the shortest deformation from one curve to another

Starting from a point $c_0 \in \mathcal{C}$, "shoot" in the direction u_0, then adjust u_0 until convergence.

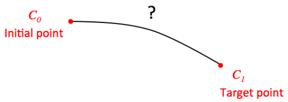

The space of curves $\mathcal{C}$

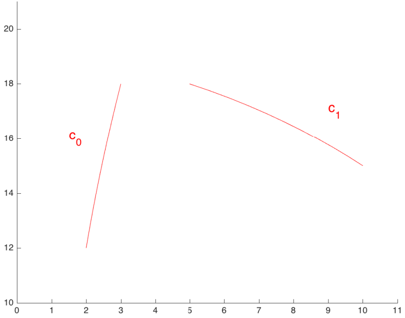

The hyperbolic upper-half plane $\mathbb{H}$

Geodesic shooting

Gives an approximation of the shortest deformation from one curve to another

Starting from a point $c_0 \in \mathcal{C}$, "shoot" in the direction u_0, then adjust u_0 until convergence.

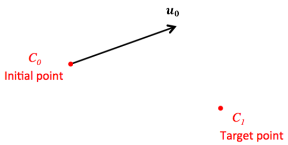

The space of curves $\mathcal{C}$

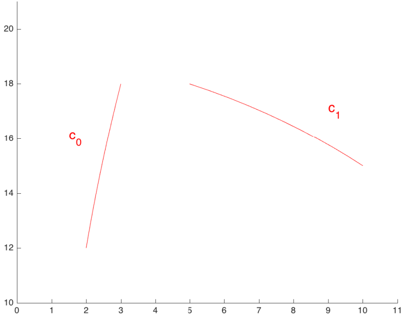

The hyperbolic upper-half plane $\mathbb{H}$

Geodesic shooting

Gives an approximation of the shortest deformation from one curve to another

Starting from a point $c_0 \in \mathcal{C}$, "shoot" in the direction u_0, then adjust u_0 until convergence.

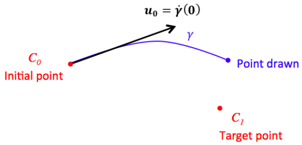

The space of curves $\mathcal{C}$

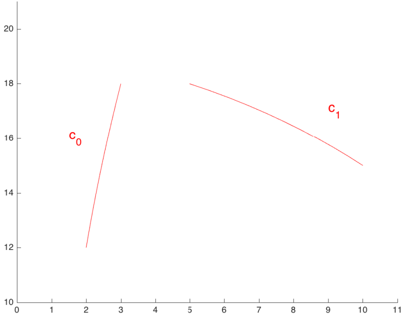

The hyperbolic upper-half plane $\mathbb{H}$

Geodesic shooting

Gives an approximation of the shortest deformation from one curve to another

Starting from a point $c_0 \in \mathcal{C}$, "shoot" in the direction u_0, then adjust u_0 until convergence.

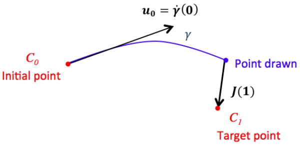

The space of curves $\mathcal{C}$

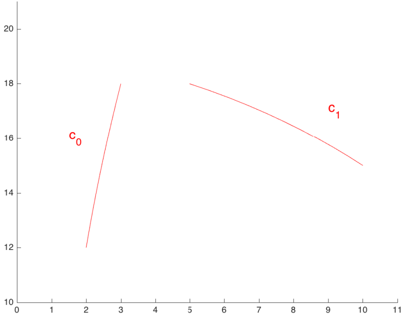

The hyperbolic upper-half plane $\mathbb{H}$

Geodesic shooting

Gives an approximation of the shortest deformation from one curve to another

Starting from a point $c_0 \in \mathcal{C}$, "shoot" in the direction u_0, then adjust u_0 until convergence.

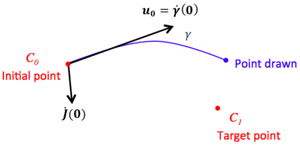

The space of curves $\mathcal{C}$

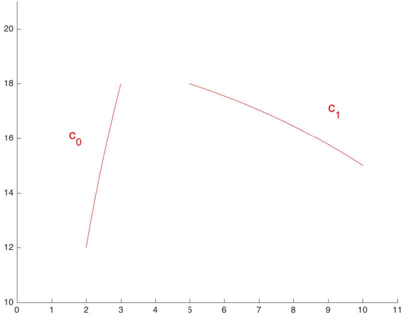

The hyperbolic upper-half plane $\mathbb{H}$

Geodesic shooting

Gives an approximation of the shortest deformation from one curve to another

Starting from a point $c_0 \in \mathcal{C}$, "shoot" in the direction u_0, then adjust u_0 until convergence.

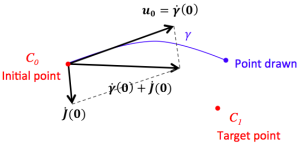

The space of curves $\mathcal{C}$

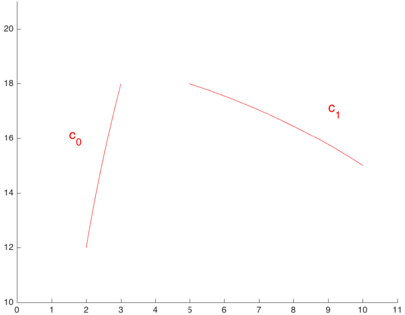

The hyperbolic upper-half plane $\mathbb{H}$

Geodesic shooting

Gives an approximation of the shortest deformation from one curve to another

Starting from a point $c_0 \in \mathcal{C}$, "shoot" in the direction u_0, then adjust u_0 until convergence.

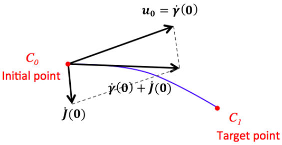

The space of curves $\mathcal{C}$

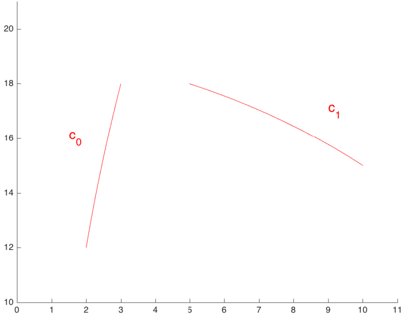

The hyperbolic upper-half plane $\mathbb{H}$

Geodesic shooting

Gives an approximation of the shortest deformation from one curve to another

Starting from a point $c_0 \in \mathcal{C}$, "shoot" in the direction u_0, then adjust u_0 until convergence.

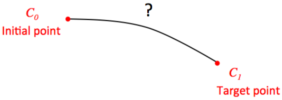

The space of curves $\mathcal{C}$

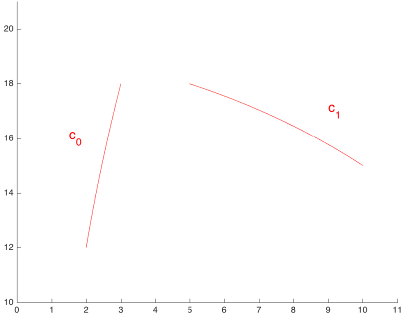

The hyperbolic upper-half plane $\mathbb{H}$

Geodesic shooting

Gives an approximation of the shortest deformation from one curve to another

Starting from a point $c_0 \in \mathcal{C}$, "shoot" in the direction u_0, then adjust u_0 until convergence.

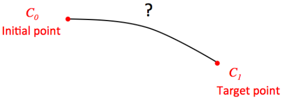

The space of curves $\mathcal{C}$

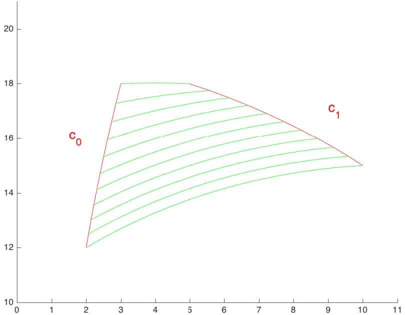

The hyperbolic upper-half plane $\mathbb{H}$

Geodesic shooting

Gives an approximation of the shortest deformation from one curve to another

Starting from a point $c_0 \in \mathcal{C}$, "shoot" in the direction u_0, then adjust u_0 until convergence.

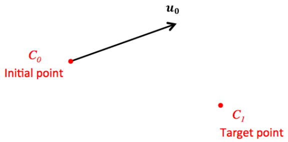

The space of curves $\mathcal{C}$

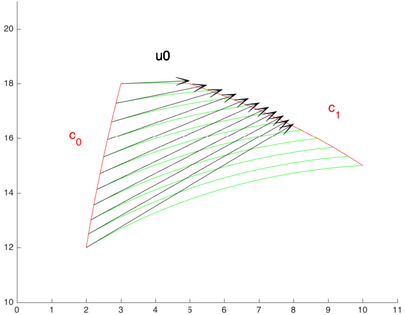

The hyperbolic upper-half plane $\mathbb{H}$

Geodesic shooting

Gives an approximation of the shortest deformation from one curve to another

Starting from a point $c_0 \in \mathcal{C}$, "shoot" in the direction u_0, then adjust u_0 until convergence.

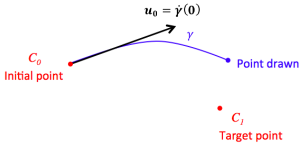

The space of curves $\mathcal{C}$

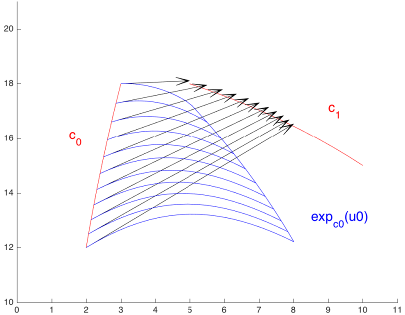

The hyperbolic upper-half plane $\mathbb{H}$

Geodesic shooting

Gives an approximation of the shortest deformation from one curve to another

Starting from a point $c_0 \in \mathcal{C}$, "shoot" in the direction u_0, then adjust u_0 until convergence.

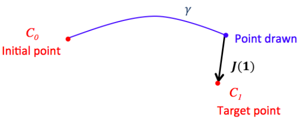

The space of curves $\mathcal{C}$

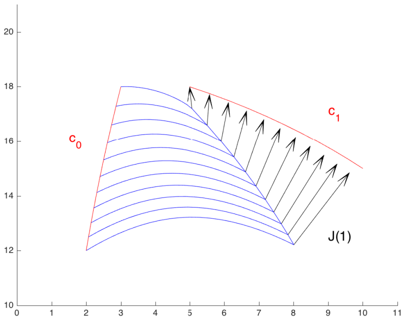

The hyperbolic upper-half plane $\mathbb{H}$

Geodesic shooting

Gives an approximation of the shortest deformation from one curve to another

Starting from a point $c_0 \in \mathcal{C}$, "shoot" in the direction u_0, then adjust u_0 until convergence.

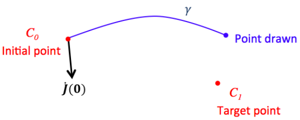

The space of curves $\mathcal{C}$

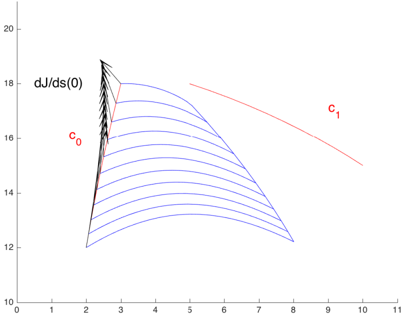

The hyperbolic upper-half plane $\mathbb{H}$

Geodesic shooting

Gives an approximation of the shortest deformation from one curve to another

Starting from a point $c_0 \in \mathcal{C}$, "shoot" in the direction u_0, then adjust u_0 until convergence.

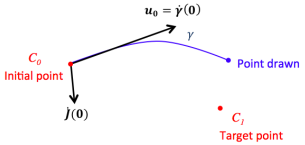

The space of curves $\mathcal{C}$

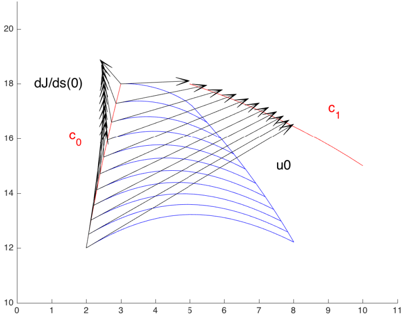

The hyperbolic upper-half plane $\mathbb{H}$

Geodesic shooting

Gives an approximation of the shortest deformation from one curve to another

Starting from a point $c_0 \in \mathcal{C}$, "shoot" in the direction u_0, then adjust u_0 until convergence.

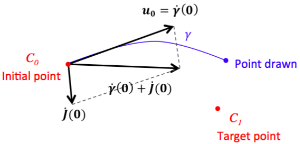

The space of curves $\mathcal{C}$

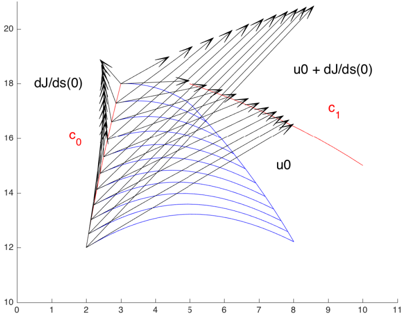

The hyperbolic upper-half plane $\mathbb{H}$

Geodesic shooting

Gives an approximation of the shortest deformation from one curve to another

Starting from a point $c_0 \in \mathcal{C}$, "shoot" in the direction u_0, then adjust u_0 until convergence.

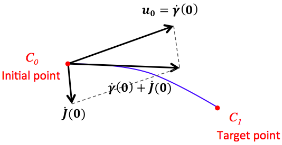

The space of curves $\mathcal{C}$

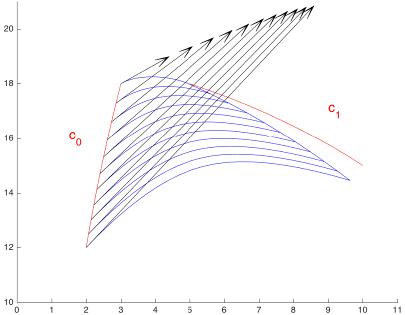

The hyperbolic upper-half plane $\mathbb{H}$

Geodesic shooting

- Gives an approximation of the shortest deformation from one curve to another
- Starting from a point $c_0 \in \mathcal{C}$, "shoot" in the direction u_0, then adjust u_0 until convergence.

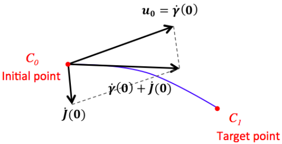

The space of curves $\mathcal{C}$

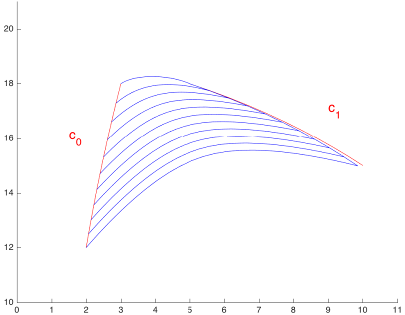

The hyperbolic upper-half plane $\mathbb{H}$

Geodesic shooting

Gives an approximation of the shortest deformation from one curve to another

Starting from a point $c_0 \in \mathcal{C}$, "shoot" in the direction u_0, then adjust u_0 until convergence.

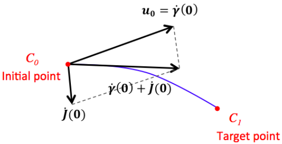

The space of curves $\mathcal{C}$

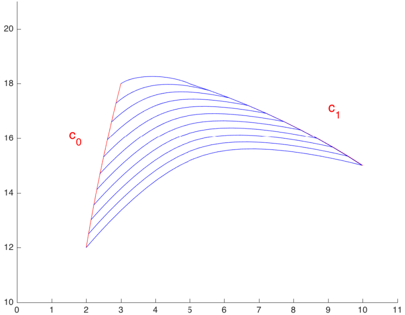

The hyperbolic upper-half plane $\mathbb{H}$

Geodesic shooting

Gives an approximation of the shortest deformation from one curve to another

Starting from a point $c_0 \in \mathcal{C}$, "shoot" in the direction u_0, then adjust u_0 until convergence.

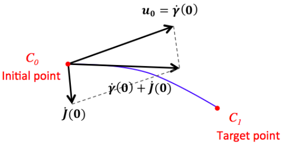

The space of curves $\mathcal{C}$

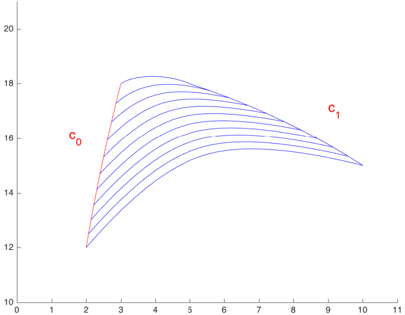

The hyperbolic upper-half plane $\mathbb{H}$

Geodesic shooting

Gives an approximation of the shortest deformation from one curve to another

Starting from a point $c_0 \in \mathcal{C}$, "shoot" in the direction u_0, then adjust u_0 until convergence.

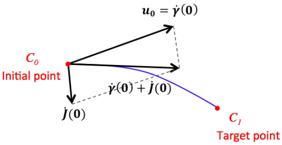

The space of curves $\mathcal{C}$

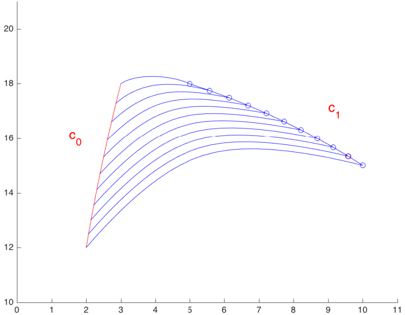

The hyperbolic upper-half plane $\mathbb{H}$

Fréchet mean

The Fréchet mean minimizes the functional $F(c) = \sum \mathrm{dist}_G^2(c_i, c)$
$\rightarrow$ the mean is updated in the direction of the opposite of the gradient $-\nabla F(c) = 2\sum \log_c c_i$

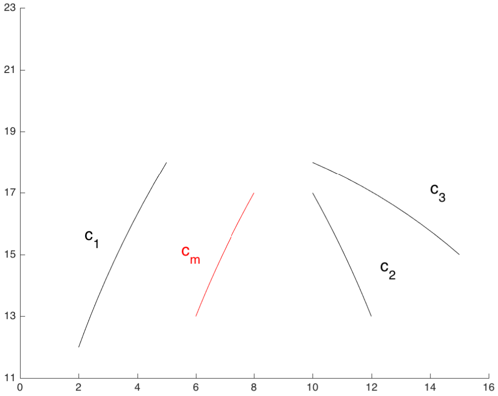

Fréchet mean

The Fréchet mean minimizes the functional $F(c) = \sum \mathrm{dist}_G^2(c_i, c)$
$\rightarrow$ the mean is updated in the direction of the opposite of the gradient $-\nabla F(c) = 2\sum \log_c c_i$

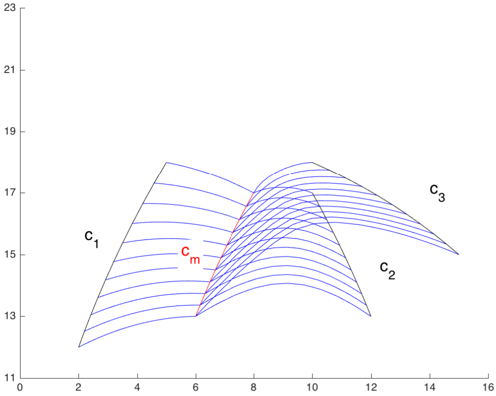

Fréchet mean

The Fréchet mean minimizes the functional $F(c) = \sum \mathrm{dist}_G^2(c_i, c)$
$\rightarrow$ the mean is updated in the direction of the opposite of the gradient $-\nabla F(c) = 2\sum \log_c c_i$

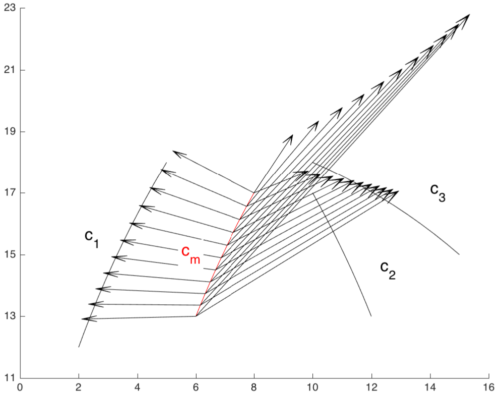

Fréchet mean

The Fréchet mean minimizes the functional $F(c) = \sum \mathrm{dist}_G^2(c_i, c)$
$\rightarrow$ the mean is updated in the direction of the opposite of the gradient $-\nabla F(c) = 2\sum \log_c c_i$

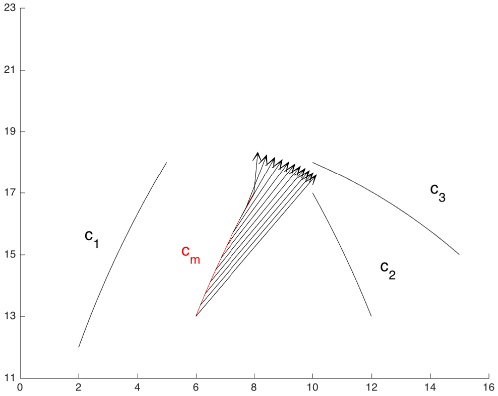

Fréchet mean

The Fréchet mean minimizes the functional $F(c) = \sum \mathrm{dist}_G^2(c_i, c)$
$\rightarrow$ the mean is updated in the direction of the opposite of the gradient $-\nabla F(c) = 2\sum \log_c c_i$

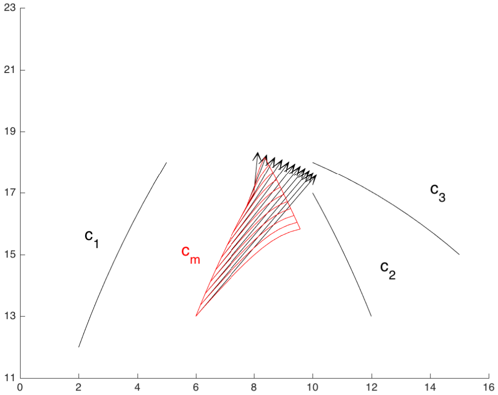

Fréchet mean

The Fréchet mean minimizes the functional $F(c) = \sum \mathrm{dist}_G^2(c_i, c)$
$\rightarrow$ the mean is updated in the direction of the opposite of the gradient $-\nabla F(c) = 2\sum \log_c c_i$

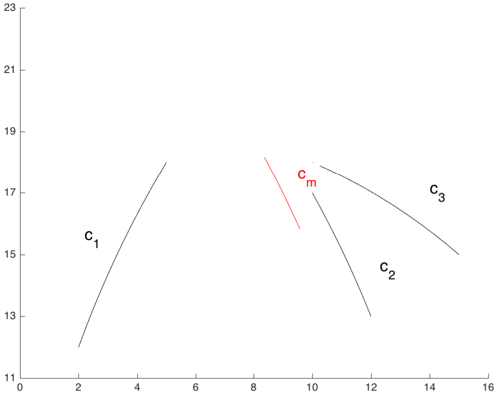

Fréchet mean

The Fréchet mean minimizes the functional $F(c) = \sum \mathrm{dist}_G^2(c_i, c)$
$\rightarrow$ the mean is updated in the direction of the opposite of the gradient $-\nabla F(c) = 2\sum \log_c c_i$

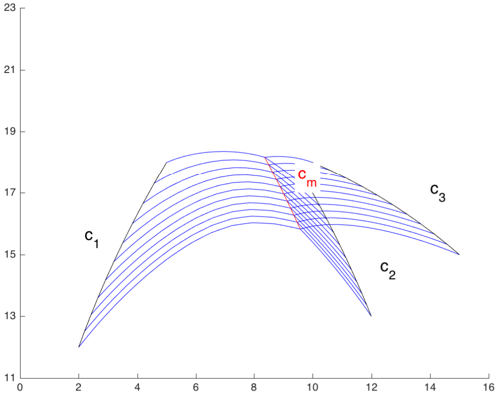

Fréchet mean

The Fréchet mean minimizes the functional $F(c) = \sum \text{dist}_G^2(c_i, c)$
$\rightarrow$ the mean is updated in the direction of the opposite of the gradient $-\nabla F(c) = 2\sum \log_c c_i$

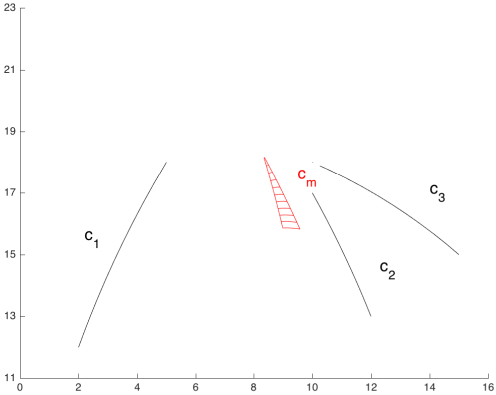

Fréchet mean

The Fréchet mean minimizes the functional $F(c) = \sum \mathrm{dist}_G^2(c_i, c)$
$\rightarrow$ the mean is updated in the direction of the opposite of the gradient $-\nabla F(c) = 2 \sum \log_c c_i$

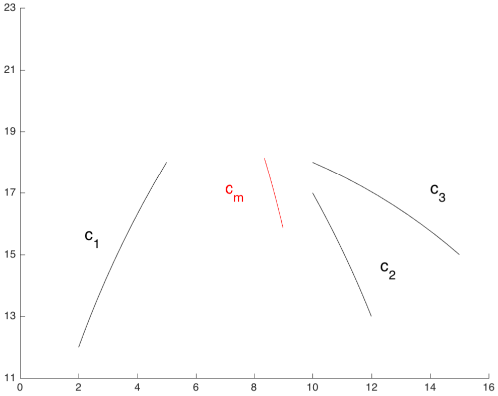

Fréchet mean

The Fréchet mean minimizes the functional $F(c) = \sum \mathrm{dist}_G^2(c_i, c)$
$\rightarrow$ the mean is updated in the direction of the opposite of the gradient $-\nabla F(c) = 2\sum \log_c c_i$

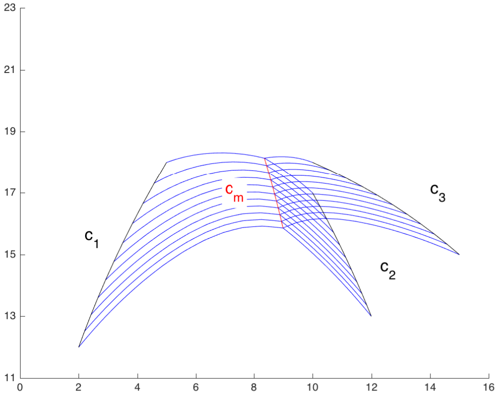

Fréchet mean

The Fréchet mean minimizes the functional $F(c) = \sum \mathrm{dist}_G^2(c_i, c)$
$\rightarrow$ the mean is updated in the direction of the opposite of the gradient $-\nabla F(c) = 2\sum \log_c c_i$

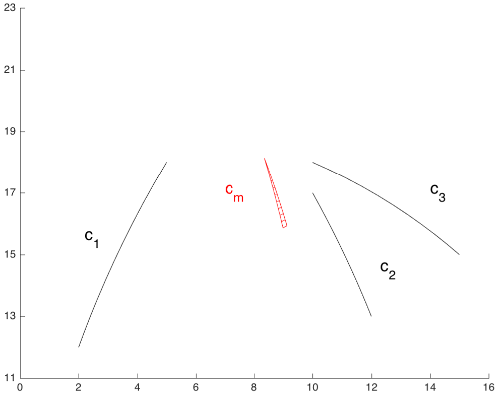

Fréchet mean

The Fréchet mean minimizes the functional $F(c) = \sum \mathrm{dist}_G^2(c_i, c)$
$\rightarrow$ the mean is updated in the direction of the opposite of the gradient $-\nabla F(c) = 2\sum \log_c c_i$

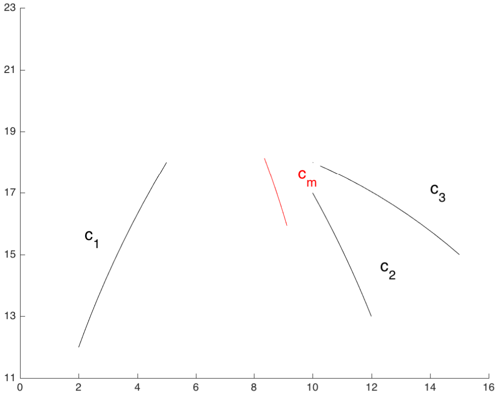

Fréchet mean

The Fréchet mean minimizes the functional $F(c) = \sum \mathrm{dist}_G^2(c_i, c)$
$\rightarrow$ the mean is updated in the direction of the opposite of the gradient $-\nabla F(c) = 2\sum \log_c c_i$

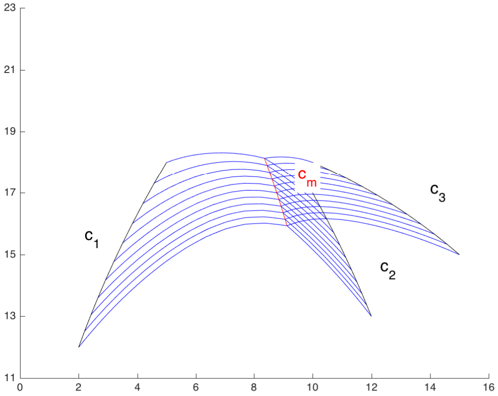

Fréchet mean

The Fréchet mean minimizes the functional $F(c) = \sum \mathrm{dist}_G^2(c_i, c)$
$\rightarrow$ the mean is updated in the direction of the opposite of the gradient $-\nabla F(c) = 2\sum \log_c c_i$

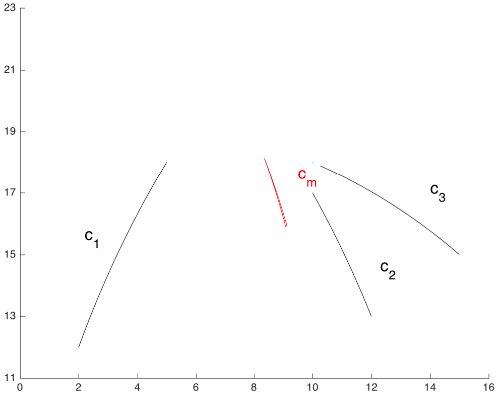

Fréchet mean

The Fréchet mean minimizes the functional $F(c) = \sum \mathrm{dist}_G^2(c_i, c)$
$\rightarrow$ the mean is updated in the direction of the opposite of the gradient $-\nabla F(c) = 2 \sum \log_c c_i$

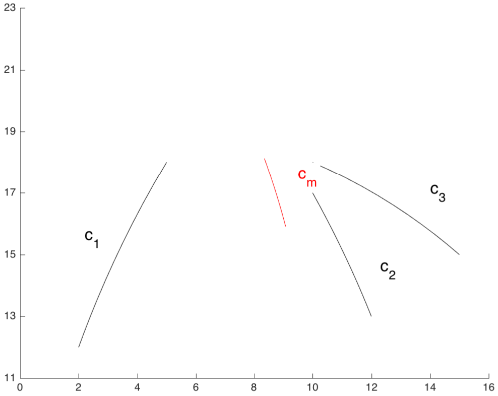

Fréchet mean

The Fréchet mean minimizes the functional $F(c) = \sum \mathrm{dist}_G^2(c_i, c)$
$\rightarrow$ the mean is updated in the direction of the opposite of the gradient $-\nabla F(c) = 2\sum \log_c c_i$

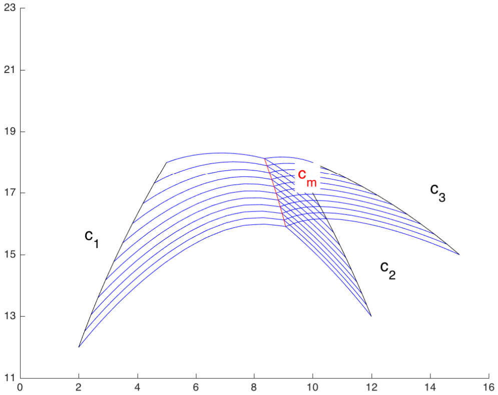

Fréchet mean

The Fréchet mean minimizes the functional $F(c) = \sum \mathrm{dist}_G^2(c_i, c)$
$\rightarrow$ the mean is updated in the direction of the opposite of the gradient $-\nabla F(c) = 2\sum \log_c c_i$

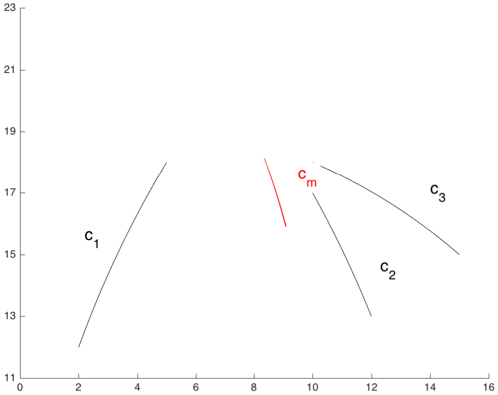

Fréchet mean

Example with helicopter data : computation of the mean of three curves

$$\mu^{370}(t), \quad \mu^{390}(t), \quad \mu^{410}(t),$$

corresponding to 3 different rotor rotation speeds $\omega = 370$ RPM, $\omega = 390$ RPM, $\omega = 410$ RPM.

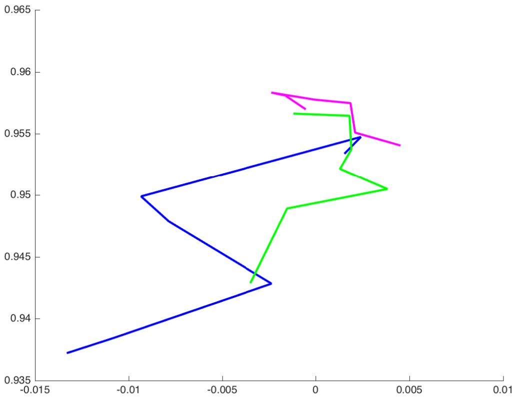

Fréchet mean

Example with helicopter data : computation of the mean of three curves

$$\mu^{370}(t), \quad \mu^{390}(t), \quad \mu^{410}(t),$$

corresponding to 3 different rotor rotation speeds $\omega = 370$ RPM, $\omega = 390$ RPM, $\omega = 410$ RPM.

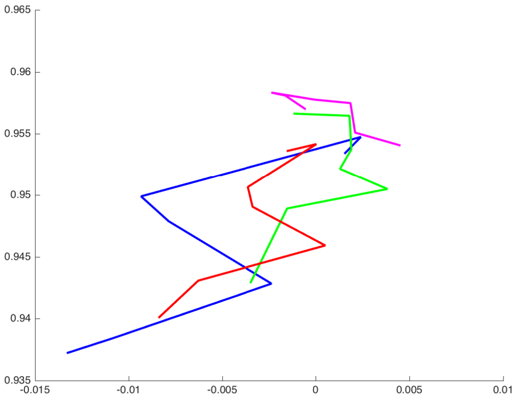

Fréchet mean

Example with helicopter data : computation of the mean of three curves

$$\mu^{370}(t), \quad \mu^{390}(t), \quad \mu^{410}(t),$$

corresponding to 3 different rotor rotation speeds $\omega = 370$ RPM, $\omega = 390$ RPM, $\omega = 410$ RPM.

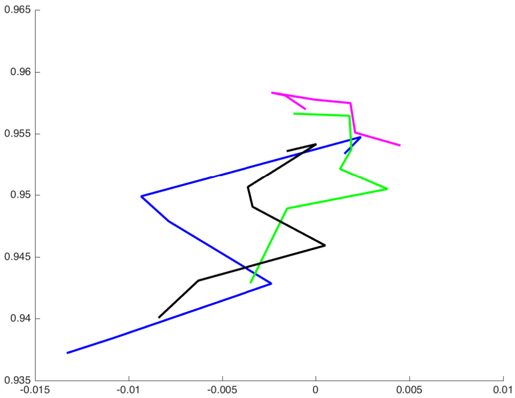

Fréchet mean

Example with helicopter data : computation of the mean of three curves

$$\mu^{370}(t), \quad \mu^{390}(t), \quad \mu^{410}(t),$$

corresponding to 3 different rotor rotation speeds $\omega = 370$ RPM, $\quad \omega = 390$ RPM, $\quad \omega = 410$ RPM.

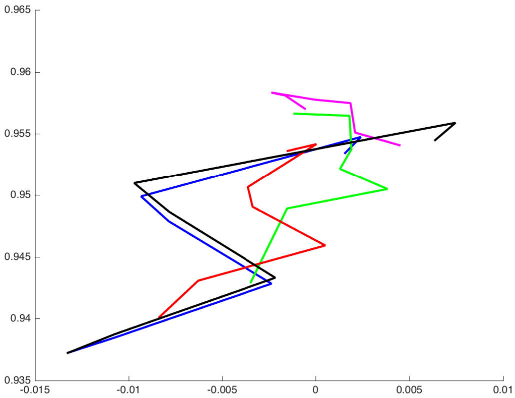

Fréchet mean

Example with helicopter data : computation of the mean of three curves

$$\mu^{370}(t), \quad \mu^{390}(t), \quad \mu^{410}(t),$$

corresponding to 3 different rotor rotation speeds $\omega = 370$ RPM, $\quad \omega = 390$ RPM, $\quad \omega = 410$ RPM.

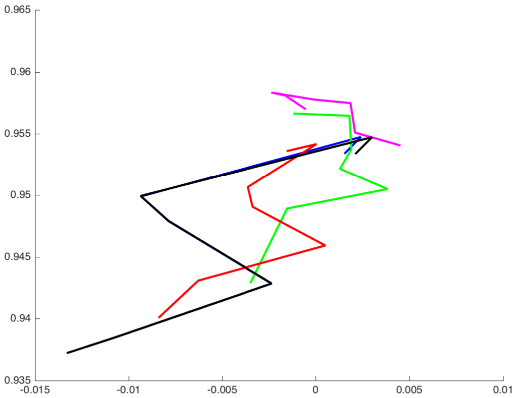

Fréchet mean

Example with helicopter data : computation of the mean of three curves

$$\mu^{370}(t), \quad \mu^{390}(t), \quad \mu^{410}(t),$$

corresponding to 3 different rotor rotation speeds $\omega = 370$ RPM, $\quad \omega = 390$ RPM, $\quad \omega = 410$ RPM.

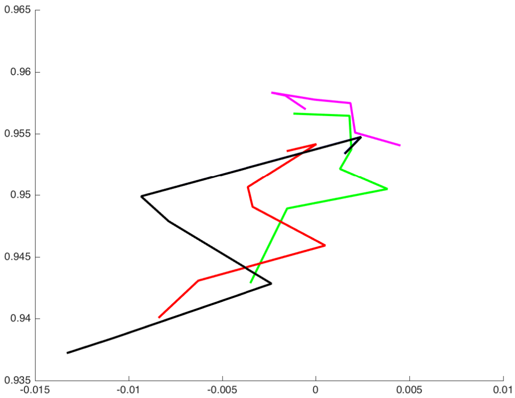

Fréchet mean

Example with helicopter data : computation of the mean of three curves

$$\mu^{370}(t), \quad \mu^{390}(t), \quad \mu^{410}(t),$$

corresponding to 3 different rotor rotation speeds $\omega = 370$ RPM, $\quad \omega = 390$ RPM, $\quad \omega = 410$ RPM.

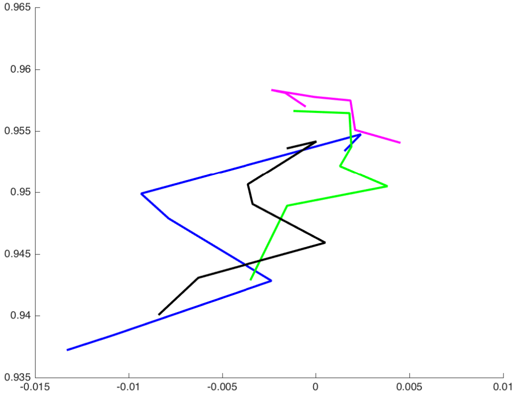

Fréchet mean

Example with helicopter data : computation of the mean of three curves

$$\mu^{370}(t), \quad \mu^{390}(t), \quad \mu^{410}(t),$$

corresponding to 3 different rotor rotation speeds $\omega = 370$ RPM, $\omega = 390$ RPM, $\omega = 410$ RPM.

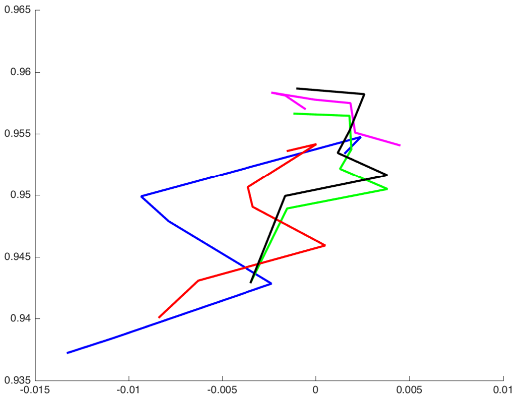

Fréchet mean

Example with helicopter data : computation of the mean of three curves

$$\mu^{370}(t), \quad \mu^{390}(t), \quad \mu^{410}(t),$$

corresponding to 3 different rotor rotation speeds $\omega = 370$ RPM, $\omega = 390$ RPM, $\omega = 410$ RPM.

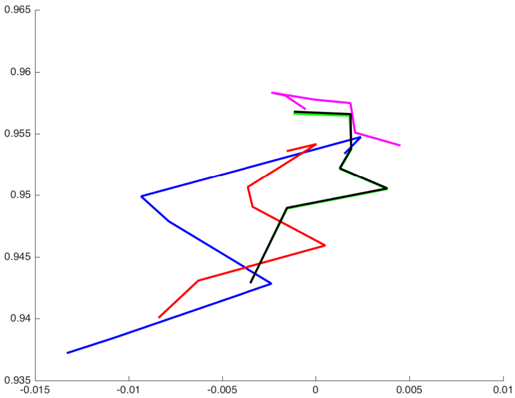

Fréchet mean

Example with helicopter data : computation of the mean of three curves

$$\mu^{370}(t), \quad \mu^{390}(t), \quad \mu^{410}(t),$$

corresponding to 3 different rotor rotation speeds $\omega = 370$ RPM, $\omega = 390$ RPM, $\omega = 410$ RPM.

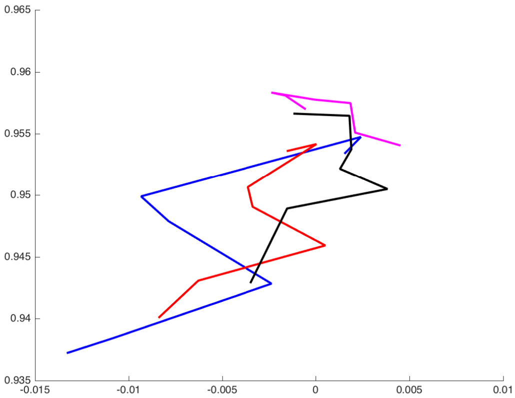

Fréchet mean

Example with helicopter data : computation of the mean of three curves

$$\mu^{370}(t), \quad \mu^{390}(t), \quad \mu^{410}(t),$$

corresponding to 3 different rotor rotation speeds $\omega = 370$ RPM, $\omega = 390$ RPM, $\omega = 410$ RPM.

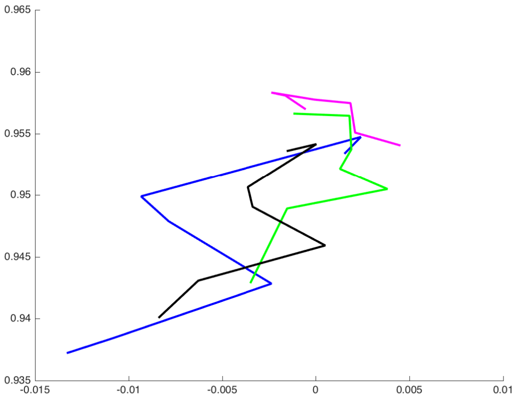

Fréchet mean

Example with helicopter data : computation of the mean of three curves

$$\mu^{370}(t), \quad \mu^{390}(t), \quad \mu^{410}(t),$$

corresponding to 3 different rotor rotation speeds $\omega = 370$ RPM, $\omega = 390$ RPM, $\omega = 410$ RPM.

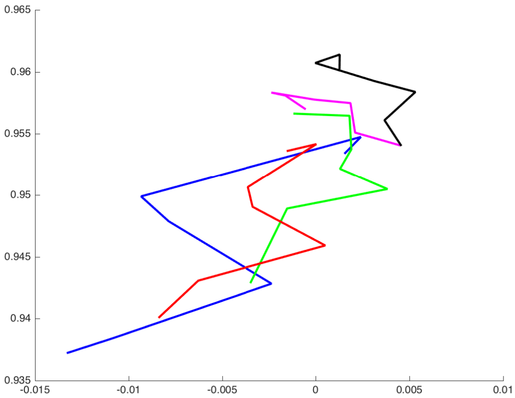

Fréchet mean

Example with helicopter data : computation of the mean of three curves

$$\mu^{370}(t), \quad \mu^{390}(t), \quad \mu^{410}(t),$$

corresponding to 3 different rotor rotation speeds $\omega = 370$ RPM, $\omega = 390$ RPM, $\omega = 410$ RPM.

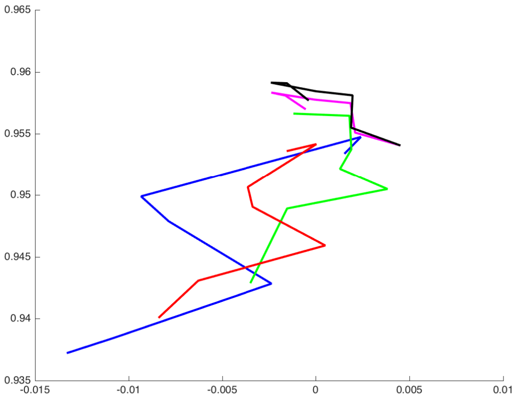

Fréchet mean

Example with helicopter data : computation of the mean of three curves

$$\mu^{370}(t), \quad \mu^{390}(t), \quad \mu^{410}(t),$$

corresponding to 3 different rotor rotation speeds $\omega = 370$ RPM, $\omega = 390$ RPM, $\omega = 410$ RPM.

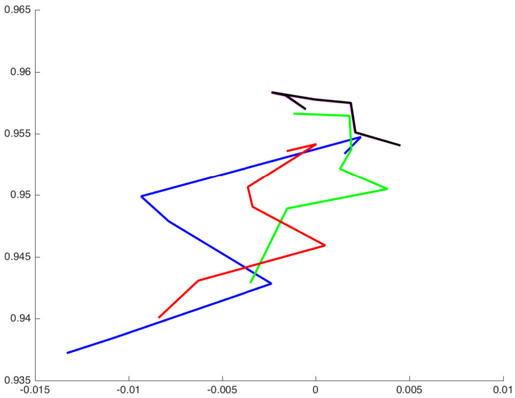

Fréchet mean

Example with helicopter data : computation of the mean of three curves

$$\mu^{370}(t), \quad \mu^{390}(t), \quad \mu^{410}(t),$$

corresponding to 3 different rotor rotation speeds $\omega = 370$ RPM, $\omega = 390$ RPM, $\omega = 410$ RPM.

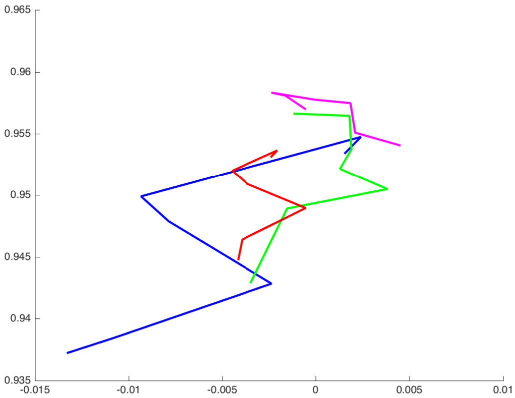

Fréchet mean

Example with helicopter data : computation of the mean of three curves

$$\mu^{370}(t), \quad \mu^{390}(t), \quad \mu^{410}(t),$$

corresponding to 3 different rotor rotation speeds $\omega = 370$ RPM, $\quad \omega = 390$ RPM, $\quad \omega = 410$ RPM.

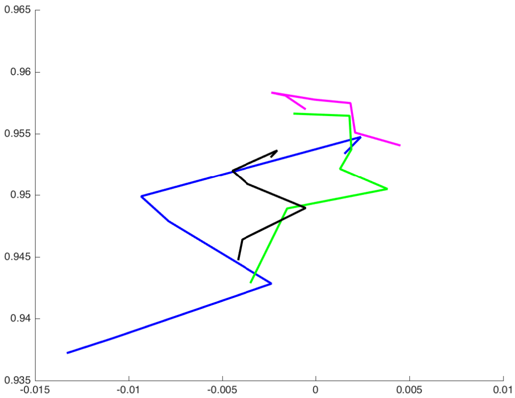

Fréchet mean

Example with helicopter data : computation of the mean of three curves

$$\mu^{370}(t), \quad \mu^{390}(t), \quad \mu^{410}(t),$$

corresponding to 3 different rotor rotation speeds $\omega = 370$ RPM, $\omega = 390$ RPM, $\omega = 410$ RPM.

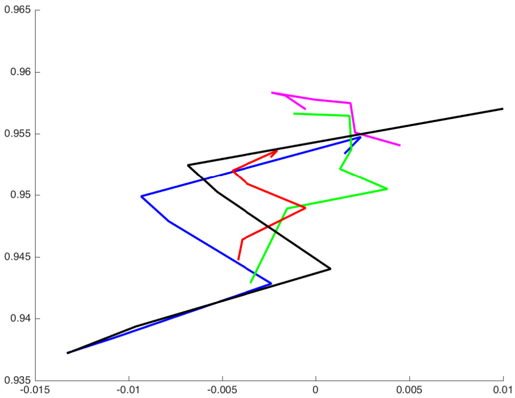

Fréchet mean

Example with helicopter data : computation of the mean of three curves

$$\mu^{370}(t), \quad \mu^{390}(t), \quad \mu^{410}(t),$$

corresponding to 3 different rotor rotation speeds $\omega = 370$ RPM, $\quad \omega = 390$ RPM, $\quad \omega = 410$ RPM.

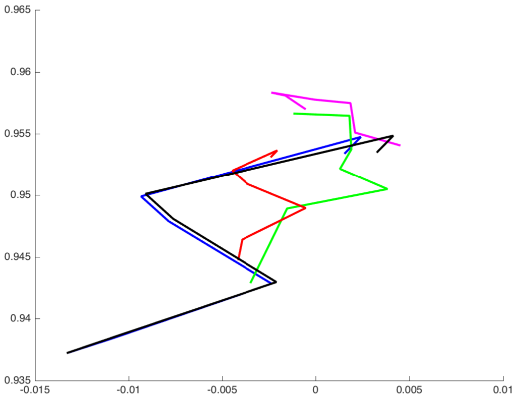

Fréchet mean

Example with helicopter data : computation of the mean of three curves

$$\mu^{370}(t), \quad \mu^{390}(t), \quad \mu^{410}(t),$$

corresponding to 3 different rotor rotation speeds $\omega = 370$ RPM, $\quad \omega = 390$ RPM, $\quad \omega = 410$ RPM.

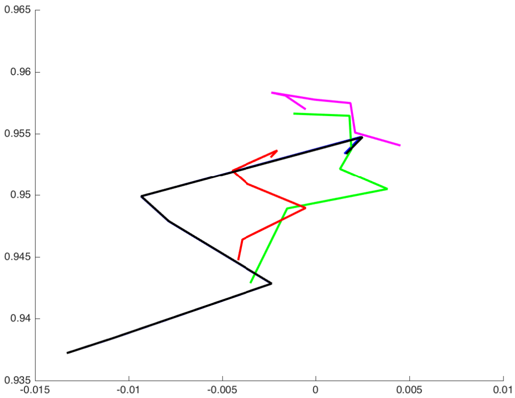

Fréchet mean

Example with helicopter data : computation of the mean of three curves

$$\mu^{370}(t), \quad \mu^{390}(t), \quad \mu^{410}(t),$$

corresponding to 3 different rotor rotation speeds $\omega = 370$ RPM, $\quad \omega = 390$ RPM, $\quad \omega = 410$ RPM.

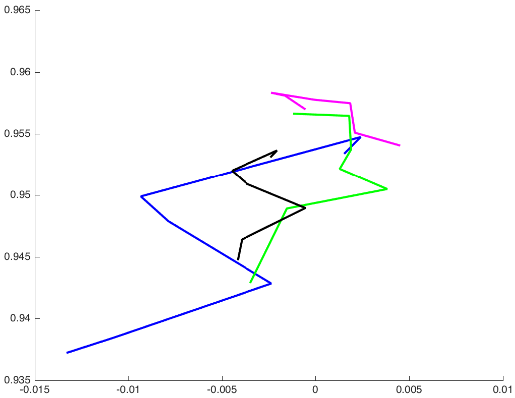

Fréchet mean

Example with helicopter data : computation of the mean of three curves

$$\mu^{370}(t), \quad \mu^{390}(t), \quad \mu^{410}(t),$$

corresponding to 3 different rotor rotation speeds $\omega = 370$ RPM, $\omega = 390$ RPM, $\omega = 410$ RPM.

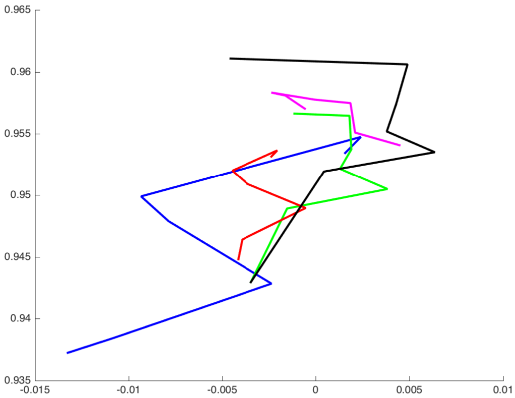

Fréchet mean

Example with helicopter data : computation of the mean of three curves

$$\mu^{370}(t), \quad \mu^{390}(t), \quad \mu^{410}(t),$$

corresponding to 3 different rotor rotation speeds $\omega = 370$ RPM, $\quad \omega = 390$ RPM, $\quad \omega = 410$ RPM.

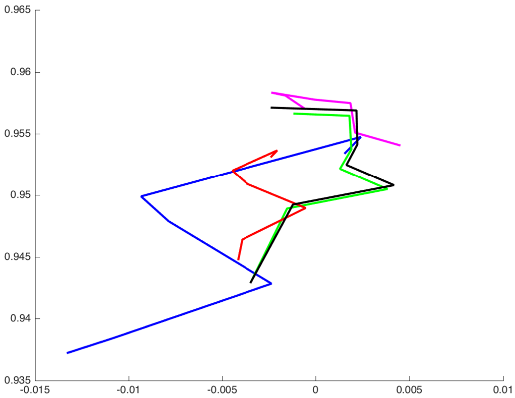

Fréchet mean

Example with helicopter data : computation of the mean of three curves

$$\mu^{370}(t), \quad \mu^{390}(t), \quad \mu^{410}(t),$$

corresponding to 3 different rotor rotation speeds $\omega = 370$ RPM, $\quad \omega = 390$ RPM, $\quad \omega = 410$ RPM.

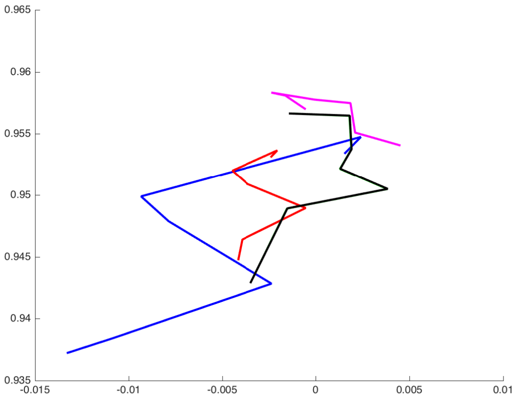

Fréchet mean

Example with helicopter data : computation of the mean of three curves

$$\mu^{370}(t), \quad \mu^{390}(t), \quad \mu^{410}(t),$$

corresponding to 3 different rotor rotation speeds $\omega = 370$ RPM, $\quad \omega = 390$ RPM, $\quad \omega = 410$ RPM.

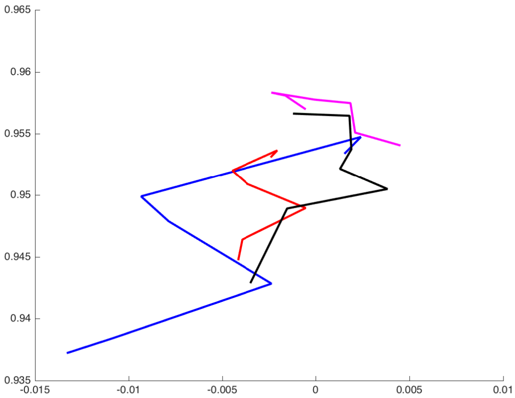

Fréchet mean

Example with helicopter data : computation of the mean of three curves

$$\mu^{370}(t), \quad \mu^{390}(t), \quad \mu^{410}(t),$$

corresponding to 3 different rotor rotation speeds $\omega = 370$ RPM, $\omega = 390$ RPM, $\omega = 410$ RPM.

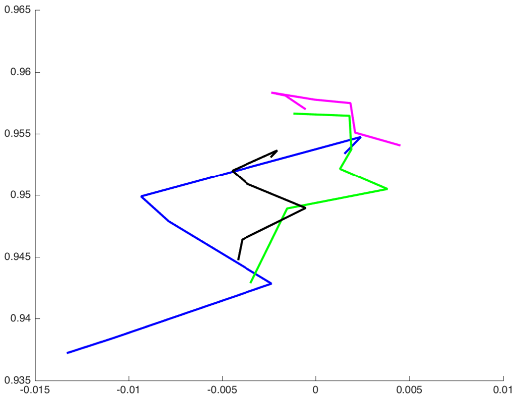

Fréchet mean

Example with helicopter data : computation of the mean of three curves

$$\mu^{370}(t), \quad \mu^{390}(t), \quad \mu^{410}(t),$$

corresponding to 3 different rotor rotation speeds $\omega = 370$ RPM, $\quad \omega = 390$ RPM, $\quad \omega = 410$ RPM.

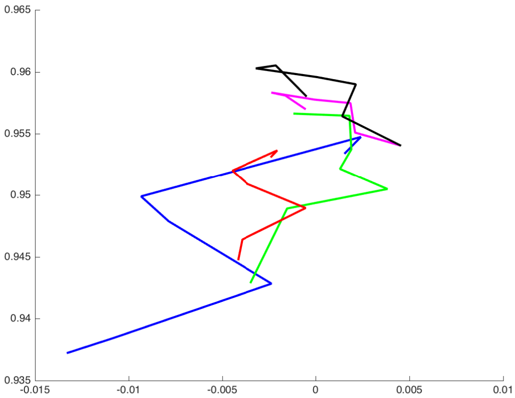

Fréchet mean

Example with helicopter data : computation of the mean of three curves

$$\mu^{370}(t), \quad \mu^{390}(t), \quad \mu^{410}(t),$$

corresponding to 3 different rotor rotation speeds $\omega = 370$ RPM, $\quad \omega = 390$ RPM, $\quad \omega = 410$ RPM.

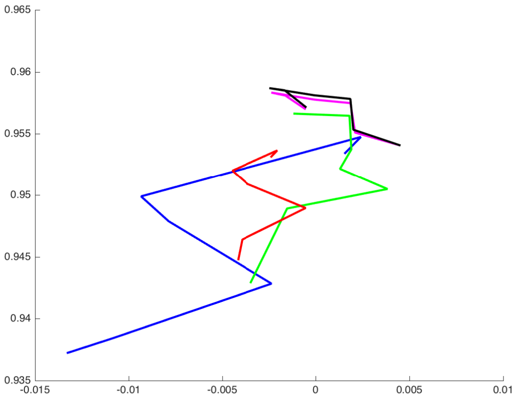

Fréchet mean

Example with helicopter data : computation of the mean of three curves

$$\mu^{370}(t), \quad \mu^{390}(t), \quad \mu^{410}(t),$$

corresponding to 3 different rotor rotation speeds $\omega = 370$ RPM, $\quad \omega = 390$ RPM, $\quad \omega = 410$ RPM.

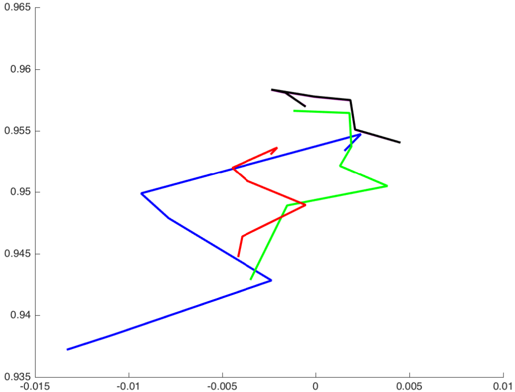

Fréchet mean

Example with helicopter data : computation of the mean of three curves

$$\mu^{370}(t), \quad \mu^{390}(t), \quad \mu^{410}(t),$$

corresponding to 3 different rotor rotation speeds $\omega = 370$ RPM, $\quad \omega = 390$ RPM, $\quad \omega = 410$ RPM.

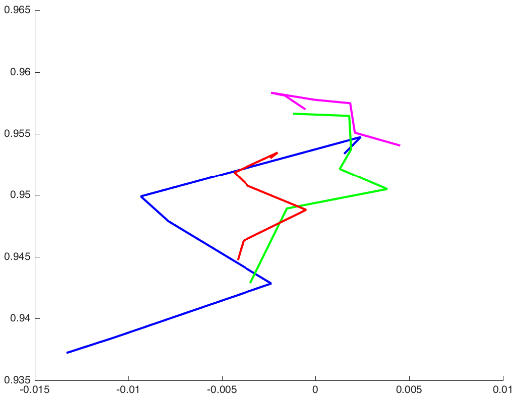

Fréchet mean

Example with helicopter data : computation of the mean of three curves

$$\mu^{370}(t), \quad \mu^{390}(t), \quad \mu^{410}(t),$$

corresponding to 3 different rotor rotation speeds $\omega = 370$ RPM, $\quad \omega = 390$ RPM, $\quad \omega = 410$ RPM.

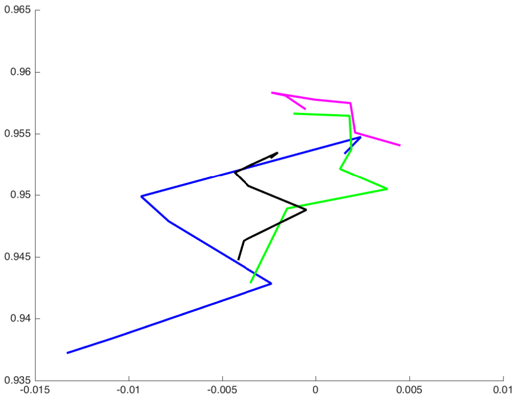

Fréchet mean

Example with helicopter data : computation of the mean of three curves

$$\mu^{370}(t), \quad \mu^{390}(t), \quad \mu^{410}(t),$$

corresponding to 3 different rotor rotation speeds $\omega = 370$ RPM, $\omega = 390$ RPM, $\omega = 410$ RPM.

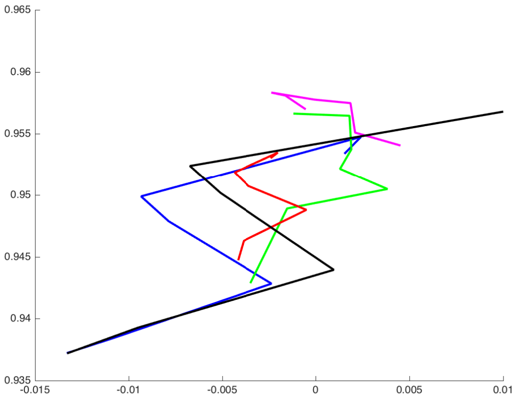

Fréchet mean

Example with helicopter data : computation of the mean of three curves

$$\mu^{370}(t), \quad \mu^{390}(t), \quad \mu^{410}(t),$$

corresponding to 3 different rotor rotation speeds $\omega = 370$ RPM, $\quad \omega = 390$ RPM, $\quad \omega = 410$ RPM.

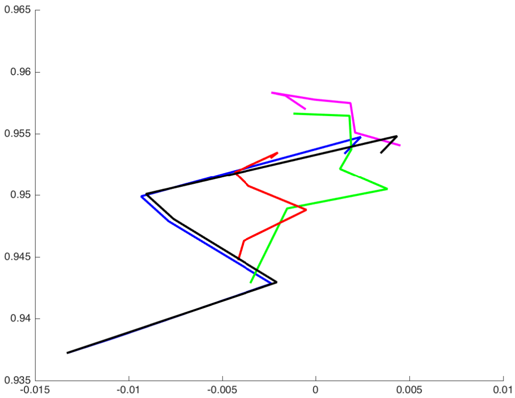

Fréchet mean

Example with helicopter data : computation of the mean of three curves

$$\mu^{370}(t), \quad \mu^{390}(t), \quad \mu^{410}(t),$$

corresponding to 3 different rotor rotation speeds $\omega = 370$ RPM, $\quad \omega = 390$ RPM, $\quad \omega = 410$ RPM.

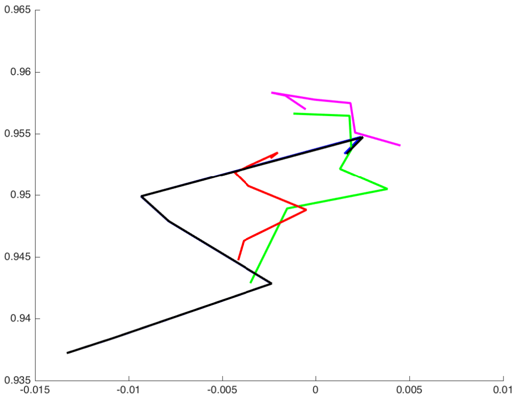

Fréchet mean

Example with helicopter data : computation of the mean of three curves

$$\mu^{370}(t), \quad \mu^{390}(t), \quad \mu^{410}(t),$$

corresponding to 3 different rotor rotation speeds $\omega = 370$ RPM, $\omega = 390$ RPM, $\omega = 410$ RPM.

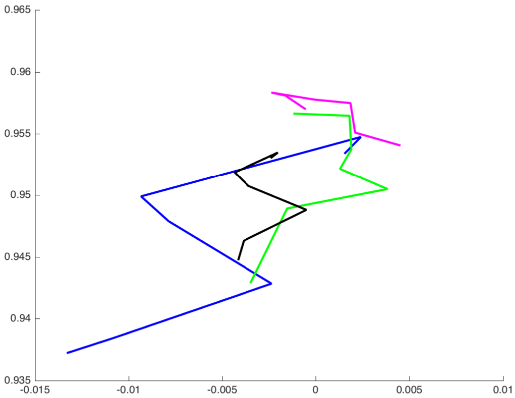

Fréchet mean

Example with helicopter data : computation of the mean of three curves

$$\mu^{370}(t), \quad \mu^{390}(t), \quad \mu^{410}(t),$$

corresponding to 3 different rotor rotation speeds $\omega = 370$ RPM, $\omega = 390$ RPM, $\omega = 410$ RPM.

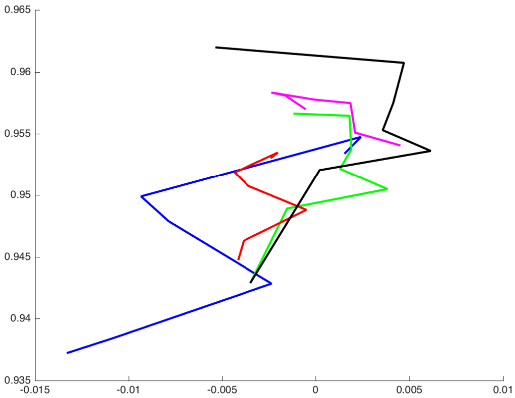

Fréchet mean

Example with helicopter data : computation of the mean of three curves

$$\mu^{370}(t), \quad \mu^{390}(t), \quad \mu^{410}(t),$$

corresponding to 3 different rotor rotation speeds $\omega = 370$ RPM, $\quad \omega = 390$ RPM, $\quad \omega = 410$ RPM.

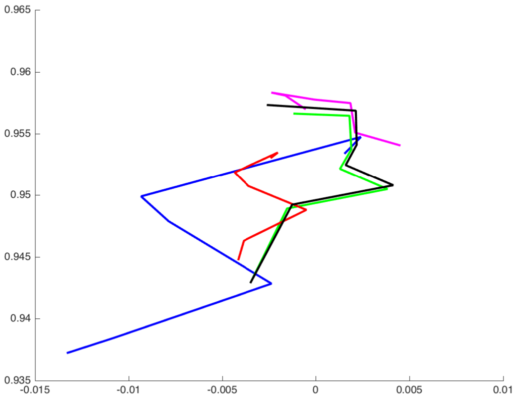

Fréchet mean

Example with helicopter data : computation of the mean of three curves

$$\mu^{370}(t), \quad \mu^{390}(t), \quad \mu^{410}(t),$$

corresponding to 3 different rotor rotation speeds $\omega = 370$ RPM, $\omega = 390$ RPM, $\omega = 410$ RPM.

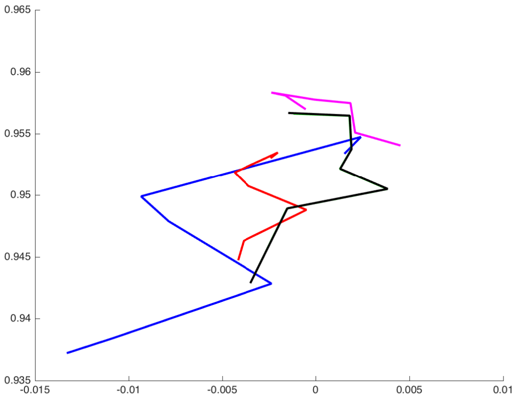

Fréchet mean

Example with helicopter data : computation of the mean of three curves

$$\mu^{370}(t), \quad \mu^{390}(t), \quad \mu^{410}(t),$$

corresponding to 3 different rotor rotation speeds $\omega = 370$ RPM, $\omega = 390$ RPM, $\omega = 410$ RPM.

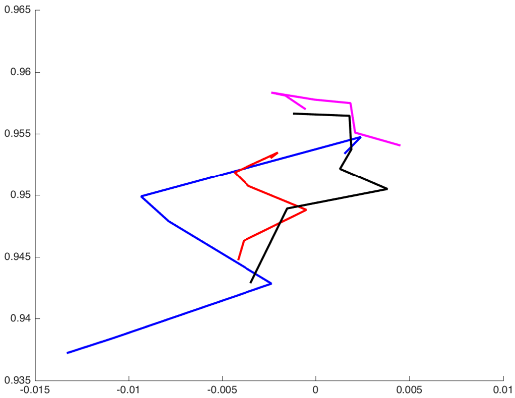

Fréchet mean

Example with helicopter data : computation of the mean of three curves

$$\mu^{370}(t), \quad \mu^{390}(t), \quad \mu^{410}(t),$$

corresponding to 3 different rotor rotation speeds $\omega = 370$ RPM, $\quad \omega = 390$ RPM, $\quad \omega = 410$ RPM.

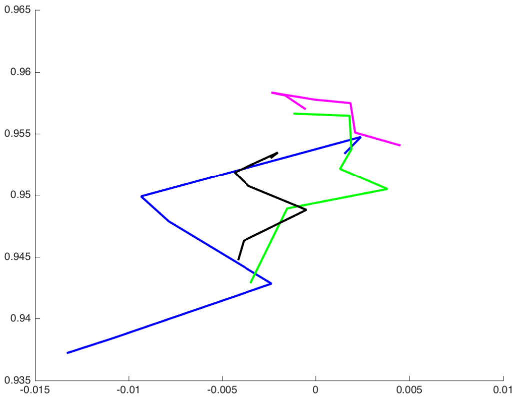

Fréchet mean

Example with helicopter data : computation of the mean of three curves

$$\mu^{370}(t), \quad \mu^{390}(t), \quad \mu^{410}(t),$$

corresponding to 3 different rotor rotation speeds $\omega = 370$ RPM, $\quad \omega = 390$ RPM, $\quad \omega = 410$ RPM.

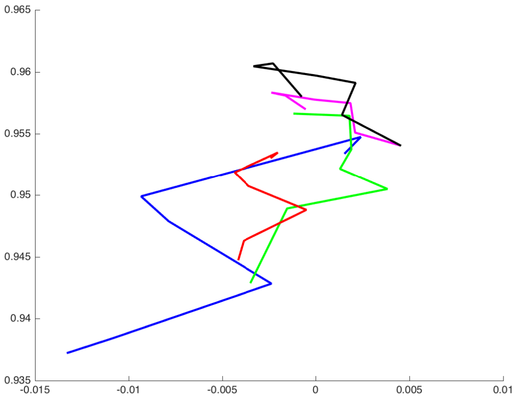

Fréchet mean

Example with helicopter data : computation of the mean of three curves

$$\mu^{370}(t), \quad \mu^{390}(t), \quad \mu^{410}(t),$$

corresponding to 3 different rotor rotation speeds $\omega = 370$ RPM, $\omega = 390$ RPM, $\omega = 410$ RPM.

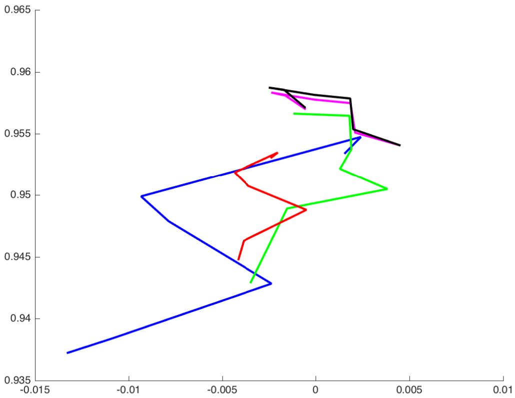

Fréchet mean

Example with helicopter data : computation of the mean of three curves

$$\mu^{370}(t), \quad \mu^{390}(t), \quad \mu^{410}(t),$$

corresponding to 3 different rotor rotation speeds $\omega = 370$ RPM, $\omega = 390$ RPM, $\omega = 410$ RPM.

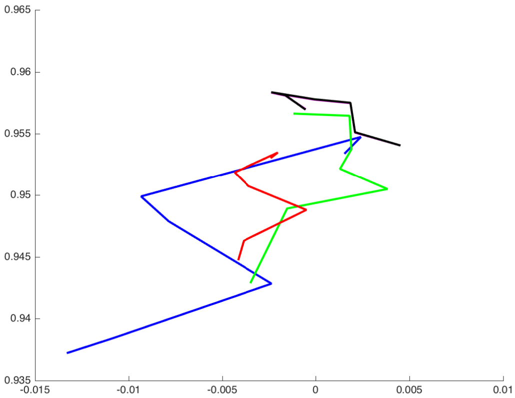

Fréchet mean

Example with helicopter data : computation of the mean of three curves

$$\mu^{370}(t), \quad \mu^{390}(t), \quad \mu^{410}(t),$$

corresponding to 3 different rotor rotation speeds $\omega = 370$ RPM, $\omega = 390$ RPM, $\omega = 410$ RPM.

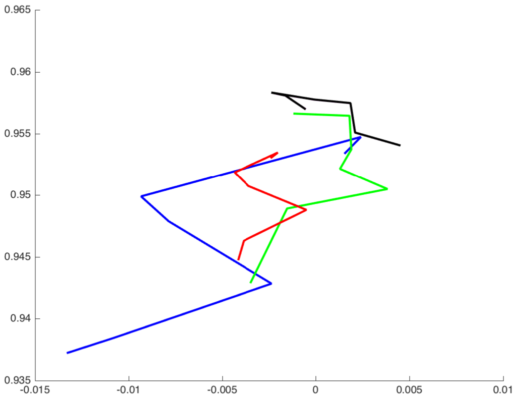

Fréchet mean

Example with helicopter data : computation of the mean of three curves

$$\mu^{370}(t), \quad \mu^{390}(t), \quad \mu^{410}(t),$$

corresponding to 3 different rotor rotation speeds $\omega = 370$ RPM, $\omega = 390$ RPM, $\omega = 410$ RPM.

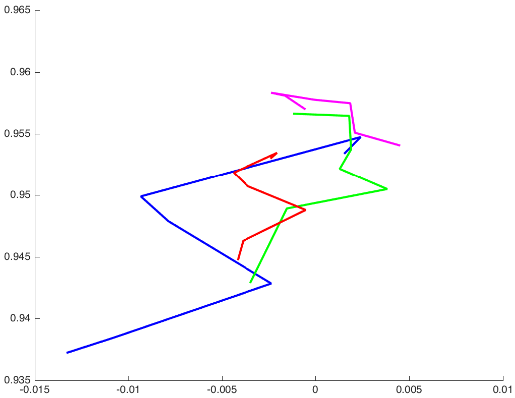

Fréchet mean

Example with helicopter data : computation of the mean of three curves

$$\mu^{370}(t), \quad \mu^{390}(t), \quad \mu^{410}(t),$$

corresponding to 3 different rotor rotation speeds $\omega = 370$ RPM, $\quad \omega = 390$ RPM, $\quad \omega = 410$ RPM.

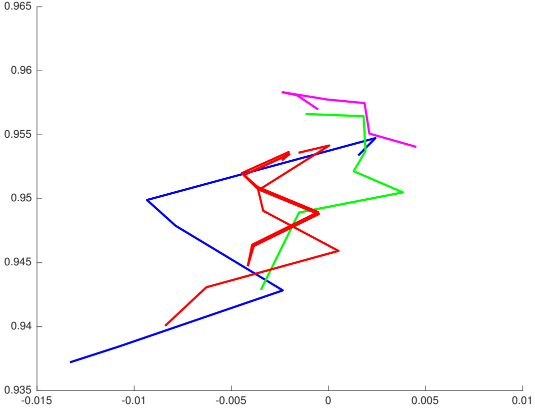

Future work

- More tests in cases where we know what to expect for a mean curve
- Study the convergence of the discrete model to the continuous model (ongoing work)
- Induce Riemannian metric on the shape space

Thank you !

Bibliography

- F. Barbaresco, Interactions between symmetric cone and information geometries. ETVC'08, Springer Lecture Notes in Computer Science (2009), 124 – 163.
- M. Bauer, M. Bruveris, S. Marsland, and P. W. Michor, Constructing reparametrization invariant metrics on spaces of plane curves. *Differential Geometry and its Applications*, 34 (2012), 139 –165.
- J. P. Burg, Maximum entropy spectral analysis. Dissertation, Stanford University (1975).
- S. I. R. Costa, S. A. Santos, and J. E. Strapasson, Fisher information distance : a geometrical reading. *Discrete Applied Mathematics*, 197 (2012).
- A. L., Computing distances and geodesics between manifold-valued curves in the SRV framework (2016), arXiv:1601.02358.
- P. W. Michor and D. Mumford, Riemannian geometries on spaces of plane curves, *Journal of the European Mathematical Society*, 8 (2006), 1 – 48.
- W. Mio, A. Srivastava, and S. Joshi. *International Journal of Comput Vision* (2007), 73: 307.
- A. Srivastava, E. Klassen, S. H. Joshi, and I. H. Jermyn. Shape analysis of elastic curves in Euclidean spaces, *IEEE Transactions on Pattern Analysis and Machine Intelligence*, 33(7) (2011), 1415 – 1428.
- L. Younes, Computable elastic distances between shapes. *SIAM Journal on Applied Mathematics*, 58 (1998), 565 – 586.
- Z. Zhang, J. Su, E. Klassen, H. Le and A. Srivastava. Video-based action recognition using rate-invariant analysis of covariance trajectories (2015), arXiv:1503.06699.